Characterization of a KDM5 Small Molecule Inhibitor with Antiviral Activity against Hepatitis B Virus

Sarah A. Gilmore[a,j], Danny Tam[a], Tara L. Cheung[a], Chelsea Snyder[a], Julie Farand[a], Ryan Dick[a,b], Mike Matles[a], Joy Y. Feng[a], Ricardo Ramirez[a], Li Li[a], Helen Yu[a], Yili Xu[a], Dwight Barnes[a], Gregg Czerwieniec[a,c], Katherine M. Brendza[a,c], Todd C. Appleby[a], Gabriel Birkus[a,d], Madeleine Willkom[a], Tetsuya Kobayashi[a], , Eric Paoli[a,e], Marc Labelle[f†], Thomas Boesen[f,g], Chin H. Tay[a,h], William E. Delaney IV[a,i], Gregory T. Notte[a], Uli Schmitz[a], and Becket Feierbach[a]

[a]Gilead Sciences, Inc., Foster City, California, USA

[b]Present address: Maze Therapeutics, South San Francisco, California, USA

[c]Present address: Nektar Therapeutics, San Francisco, CA, USA

[d]Present address: Organic Chemistry and Biochemistry of the Czech Academy of Sciences, Prague, Czech Republic

[e]Present address: Verily Life Sciences, South San Francisco, California, USA

[f] EpiTherapeutics ApS, Copenhagen, Denmark

[g] Novo Nordisk A/S, Bagsvaerd, Denmark

[h] Currently at Vir Biotechnology, San Francisco California, USA

[i] Currently at Assembly Biosciences, South San Francisco California, USA

[j] Currently at Allovir, Waltham, MA 02451

†Deceased. M.L. passed away before the submission of the final version of this manuscript. U.S. accepts responsibility for the integrity and validity of the data collected and analyzed.

26 Running title: Characterization of an HBV Antiviral Inhibitor

27

28 Abstract

29 Chronic hepatitis B (CHB) is a global health care challenge and a major cause of liver disease.
30 To find new therapeutic avenues with a potential to functionally cure chronic Hepatitis B virus
31 (HBV) infection, we performed a focused screen of epigenetic modifiers to identify replication
32 inhibitors. From this work we identified isonicotinic acid inhibitors of the histone lysine
33 demethylase 5 (KDM5) with potent anti-HBV activity. To enhance the cellular permeability and
34 liver accumulation of the most potent KDM5 inhibitor identified (GS-080) an ester prodrug was
35 developed (GS-5801) that resulted in improved bioavailability and liver exposure as well as an
36 increased H3K4me3:H3 ratio on chromatin. GS-5801 treatment of HBV-infected primary human
37 hepatocytes inhibited HBV replication and antigen levels. Evaluation of GS-5801 antiviral
38 activity in a humanized mouse model of HBV infection, however, did not result in antiviral
39 efficacy, despite achieving pharmacodynamic levels of H3K4me3:H3 predicted to be efficacious
40 from the in vitro model. Here we discuss potential reasons for the disconnect between in vitro
41 and in vivo efficacy, which highlight the translational difficulties of epigenetic targets for viral
42 diseases.

43

44 Introduction

45 Chronic hepatitis B (CHB) is a major global health care challenge and one of the main causes of
46 liver diseases including cirrhosis and hepatocellular carcinoma (HCC). Of the estimated 2 billion
47 people acutely infected with Hepatitis B virus (HBV), approximately 240 million people develop
48 CHB and 880,000 people die annually of complications from CHB [1-3]. Nucleos(t)ide

49 analogues and interferon-α (IFN-α) are approved treatments for CHB and result in suppression
50 of viral replication; however, current treatment regimens rarely result in a functional cure [4].
51 Thus, novel antiviral therapies that can cure CHB patients are needed.
52
53 HBV is a small 3.2 kb DNA virus that infects hepatocytes in the human liver. Upon infection of
54 hepatocytes, the HBV genome enters the nucleus and is converted into covalently closed circular
55 DNA (cccDNA). cccDNA is a stable, chromatinized episome that serves as the template from
56 which all viral RNA is transcribed [5, 6]. Nucleos(t)ide and IFN-α therapies do not directly
57 target cccDNA and existing long-term therapy fails to significantly impact cccDNA reservoirs in
58 the majority of patients [4, 7]. Therefore, strategies that eliminate cccDNA or effectively silence
59 the transcription of viral antigens are needed.
60
61 Emerging evidence suggests that the transcription of cccDNA is governed by the accessibility of
62 its chromatin structure. Further, posttranslational modification of histones dynamically regulates
63 cccDNA structure [8-11], akin to the well-studied epigenetic regulation of eukaryotic genomes
64 [12]. Agents that interfere with the epigenetic control of cccDNA may disrupt transcription and
65 subsequently prevent the production of viral antigens leading to a functional cure of CHB. To
66 this end, we embarked on a screen in a primary human hepatocyte (PHH) model of HBV
67 infection for compounds that repressed cccDNA transcription using a focused library of known
68 epigenetic modulators [13]. From this screen we identified two classes of small molecules with
69 antiviral activity against HBV, retinoids (ref) and inhibitors of lysine demethylase 5 (KDM5).
70

71 The KDM5 family (KDM5A – D or JARID1A – D) is a member of the Jumonji C (JmjC)
72 domain containing demethylases, which catalyze the demethylation of histones in an iron (II) and
73 α-ketoglutarate dependent manner [14, 15]. KDM5 specifically demethylates the mono-, di-, and
74 trimethylated lysine 4 residue of histone 3 in nucleosomes (H3K4me, H3K4me2, and H3K4me3)
75 (see **Fig 1A**) [16, 17]. In eukaryotic genomes, H3K4me3 is predominantly localized at the
76 transcription start sites (TSS) of highly-expressed genes, where it plays a role in RNA
77 polymerase II binding and target gene activation [18-22]. KDM5 family members are predicted
78 to act as transcriptional repressors based on the presence of H3K4me3 at the promoters of most
79 actively transcribed genes [23]. However, KDM5 may serve a broader function to promote
80 appropriate transcription by demethylating H3K4 in gene bodies thereby focusing H3K4
81 methylation at TSS [23, 24]. Accordingly, KDM5 has become an important oncology target as is
82 evident from several dozen of inhibitor patents and other publications [25, 26].
83
84 **Fig 1. GS-5801 is a prodrug of KDM5 inhibitor GS-080** (A) KDM5 demethylates the lysine 4
85 of the histone 3 (H3K4) subunit of nucleosomes. Inhibition of KDM5 activity by compounds
86 such as GS-5801 results in accumulation of methylated H3K4 on chromatin through the activity
87 of cellular histone methyltransferases (HMT) that catalyze the mono-, di-, and tri- methylation of
88 H3K4. Chemical structures of prodrug GS-5801 and parent GS-080 (B) as well as prodrug GS-
89 420 and parent GS-444 (C) are shown.
90
91 In this work we describe the discovery that a potent small molecule inhibitor of KDM5, termed
92 GS-080 [27-30], has antiviral activity against HBV in a PHH infection model. An ethyl ester
93 prodrug of GS-080 (Fig. 1), termed GS-5801, was utilized to increase the cellular permeability,

94 oral bioavailability, and liver-loading of the parent GS-080 molecule. Treatment of HBV-
95 infected PHH with GS-5801 causes accumulation of H3K4me3 relative to total H3
96 (H3K4me3:H3 ratio) on cellular DNA that correlates with a reduction in HBV RNA, DNA, and
97 antigens. In vivo studies in rats and cynomolgus monkeys show that GS-5801 is well-tolerated
98 and selectively promotes the increase of the H3K4me3:H3 ratio in the liver to a greater extent
99 than other tissues. Evaluation of GS-5801 antiviral activity in a humanized mouse model of
100 HBV-infection, however, did not result in efficacy at doses predicted to be efficacious based on
101 GS-5801 in vitro antiviral activity and pharmacodynamics (H3K4me3:H3). Together these data
102 highlight discordance between the antiviral effects of GS-5801 observed in HBV-infected
103 primary human hepatocytes and a humanized mouse model of HBV infection. Understanding the
104 translatability of therapeutic agents in HBV infection models to chronic hepatitis B infection is
105 valuable, especially given the limited number of host targets that have been evaluated clinically
106 in CHB patients. Despite a high risk of the in vivo study predicting lack of clinical efficacy, we
107 pursued the evaluation ofGS-5801 in Phase 1a and Phase 1b clinical trials for chronic hepatitis B
108 . As GS-5801 is still the first and only KDM5 inhibitor to have reached the clinic, our experience
109 underscores the translational challenges with epigenetic targets.
110
111 ## Results
112
113 **GS-5801 inhibits HBV RNA, DNA, and antigens in primary human hepatocytes**
114 To identify small molecule compounds capable of inhibiting HBV transcription, a targeted
115 library of epigenetic modifiers was evaluated in HBV-infected PHH to identify compounds that
116 reduced HBV intracellular RNA and secreted antigens: hepatitis B virus e antigen (HBeAg) and
117 hepatitis B virus s antigen (HBsAg). From this screen we identified nicotinic acid derivative
118 GS-080, and its more cell-permeable prodrug GS-5801 (see **Fig 1B**) [27-30], as inhibitors of

119 HBV RNA and antigen production in HBV-infected PHH. Importantly, neither GS-5801 nor
120 GS-080 had measurable cytotoxicity in PHH or in a panel of human cells at concentrations up to
121 57 μM (see **S1 Table**).
122
123 To further characterize the antiviral activity of GS-5801, PHH were infected with HBV
124 (genotype D; GTD) for three days prior to initiation of GS-5801 dosing. HBV-infected PHH
125 received a dose of GS-5801 every three to four days for a total of four doses over 14 days. HBV
126 intracellular RNA, extracellular DNA, and secreted HBsAg and HBeAg were measured on Day
127 14 (time post-initiation of dosing). GS-5801 EC_{50} values ranged between 0.034 – 1.1 μM
128 (median EC_{50} = 0.16 μM) for intracellular RNA, 0.0071 – 1.3 μM (median EC_{50} = 0.14 μM) for
129 extracellular DNA, 0.015 – 1.7 μM (median EC_{50} = 0.24 μM) for secreted HBsAg, and 0.014 –
130 1.1 μM (median EC_{50} = 0.15 μM) for secreted HBeAg in PHH with no cytotoxicity (CC_{50} > 10
131 μM) in the seven PHH donors tested (**Table 1**). As a negative control, GS-444, a bromo-
132 derivative of GS-080 with vastly reduced KDM5 inhibitory activity (GS-444 IC_{50} for KDM5B =
133 2760 nM; 7000-fold reduced over GS-080), was administered to PHH as its cell-permeable pro-
134 drug GS-420 (**Fig 1C**). GS-420 did not exhibit HBV antiviral activity in PHH at concentrations
135 up to 10 μM (**S2 Table**).
136
137 Amounts of cccDNA, the DNA template for transcription of HBV antigens and pre-genomic
138 RNA, were measured to determine whether the inhibition of intracellular HBV RNA,
139 extracellular DNA, and secreted antigens by GS-5801 in PHH was due to a reduction in cccDNA
140 levels. PHH were infected with HBV (genotype D; GTD) and cccDNA was established for three
141 days prior to initiation of GS-5801 dosing with compound replenishment every three to four days
142 for 14 days. Examination of cccDNA levels by Southern blot in PHH treated with GS-5801

143 indicated that GS-5801 did not alter levels of cccDNA out to 14 days of compound treatment (**SI**
144 **Fig 1**). Thus GS-5801-mediated inhibition of intracellular HBV RNA and antigen secretion is
145 not due to a reduction in levels of cccDNA.
146

147 **GS-5801 exhibits antiviral activity across HBV genotypes**

148 HBV has been classified phylogenetically into nine major genotypes, A – J, that exhibit between
149 4 – 8 % nucleotide divergence as well as distinct geographical distributions [31]. To examine
150 whether GS-5801 exhibited antiviral activity against HBV genotypes in addition to GTD, PHH
151 were infected with patient sera from individuals infected with GTA, GTC, or GTE HBV
152 genotypes that had previously been established as infectious in PHH. Following 14 days of
153 dosing, GS-5801 reduced intracellular HBV RNA (median EC_{50} = 1.1 μM, range across
154 genotypes = 0.051 – 2.7 μM), extracellular HBV DNA (median EC_{50} = 0.20 μM, range across
155 genotypes = 0.079 – 0.25 μM), and secreted HBV antigens HBsAg (EC_{50} = 0.17 μM, range
156 across genotypes = 0.036 – 3.1 μM) and HBeAg (median EC_{50} = 1.1 μM, range across genotypes
157 = 0.30 – 1.4 μM; **Table 2**) in all genotypes examined.
158

159 **GS-080 is a potent and selective inhibitor of KDM5**

160 The inhibitory activity of GS-080, the active parent of the prodrug GS-5801, was examined for
161 all four members of the KDM5 family (KDM5A – D) by in vitro biochemical characterization.
162 As summarized in **Table 1**, GS-080 had the highest inhibitory activity against KDM5A and
163 KDM5B enzymes, with IC_{50} values of 0.36 nM against KDM5A and 0.38 nM against KDM5B.
164 To assess off-target effects of GS-080, the inhibitory activity of GS-080 was examined against
165 other KDM enzymes including: KDM1, 2, 3, 4, 6, and 7 as well as a panel of HMT and HDAC

166 enzymes (see **S3 Table**). Measured GS-080 IC_{50} values for all KDM enzymes were compared to
167 the IC_{50} value of GS-080 against KDM5A to calculate the fold selectivity for each KDM enzyme
168 assayed (**Table 1**). GS-080 showed at least a 13-fold selectivity for KDM5A and KDM5B over
169 members of the KDM4 family of enzymes, and a selectivity from > 1,100- to > 278,000-fold
170 over members of the other KDM enzyme families tested. GS-080 showed no measurable
171 inhibitory activity against any of the HMT or HDAC enzymes tested (**S3 Table**; IC_{50} values >
172 100 μM). Previously characterized KDM, HDAC, or HMT inhibitors were used as positive
173 controls for the biochemical assay and included S2101, 2,4-Pyridinedicarboxylic acid (PDCA),
174 8-hydroxy-5-quinolinecarboxylic acid (IOX1), and 8-hydroxyquinoline (8-OH Quinoline), which
175 yielded IC_{50} values consistent with literature [32, 33] (**Table 1**; **S3 Table**).
176
177 **Table 1. Biochemical potency and selectivity of GS-080 against KDM enzymes.**

KDM Enzyme	Enzyme Concentration (nM)	Positive Controls IC_{50} (nM)[a]	IC_{50} (nM)[b]	Fold Selectivity Compared to KDM5A[c]
KDM5A	2.5	PDCA (410)	0.36	1
KDM5B	1.2	PDCA (410)	0.38	1
KDM5C	1	IOX1 (990)	3.7	10
KDM5D	5.5	PCDA (75)	66	183
KDM4A	0.2	PDCA (870)	7.2	20
KDM4B	1	PDCA (860)	4.7	13
KDM4C	1	PDCA (510)	4.8	13
KDM1A	0.25	S2101 (2000)	> 100,000	> 278,000
KDM2B	2	PDCA (19000)	620	> 1,720
KDM3A	0.3	IOX1 (140)	1,700	> 4,720
KDM3B	0.1	PDCA (7900)	> 10,000	> 27,800
KDM6A	2	PDCA (99000)	6,200	> 17,200
KDM6B	1	8-OH Quinoline (6400)	6,200	> 17,200
KDM7B	2.5	8-OH Quinoline (13000)	400	> 1,110

178 a The IC_{50} values of positive control compounds are shown in parentheses.

179 b The IC_{50} values for KDM enzymes represent at least n = 2 experiments. The IC_{50} values of KDM5A and KDM5B were
180 significantly lower than the enzyme concentration, indicating they likely underestimate compound potency since the assay
181 may approach its lower limit.

182 c Fold selectivity is defined by IC_{50} of KDM enzyme over KDM5A.

183

184 **Depletion of *KDM5* by siRNA restricts HBV replication in PHH**

185 To confirm that the antiviral activity we observed with the small molecule GS-5801 was due to
186 inhibition of KDM5 in PHH, we examined the effect of depleting *KDM5* transcripts by RNA
187 interference on HBV RNA and antigen production. Three days post HBV infection, *KDM5*
188 transcripts were depleted with small interfering RNA (siRNA) two times during the infection
189 time course to maintain transcript knockdown: once on Day 0 (three days post-infection) and
190 again on Day 6 (nine days post-infection). *KDM5* transcripts were depleted with siRNA either
191 individually to reduce levels of a single *KDM5* (*KDM5A, B, C,* or *D*) transcript or pooled to
192 reduce levels of *KDM5A – D* transcripts in the cell. Thirteen days after initiation of siRNA
193 treatment, amounts of *KDM5* transcripts as well as HBV RNA along with secreted antigens were
194 measured by qRT-PCR or immunoassay, respectively. siRNA knockdown of *KDM5* transcripts
195 individually (*KDM5A*, *B*, *C*, or *D*) or simultaneously (*KDM5A – D*) resulted in 55 – 78 %
196 inhibition of *KDM5* transcript levels in PHH (**SI Fig. 2A, B**) with no effect on cell viability as
197 assessed by alamarBlue staining (**SI Fig. 2D**). Knockdown of *KDM5A*, *KDM5B*, *KDM5C*, or
198 *KDM5D* transcripts individually in PHH resulted in mild repression of HBV RNA (26 – 43%),
199 HBeAg (32 – 39%), and HBsAg (34 – 41%) by Day 13 after initiation of siRNA treatment (**Fig
200 2**). In contrast, simultaneous knockdown of *KDM5A*, *KDM5B*, *KDM5C*, and *KDM5D* transcripts
201 in PHH resulted in much greater repression of HBV RNA (88 %), HBeAg (95 %), and HBsAg
202 (84 %) by Day 13 (**Fig 2**). Knockdown of *KDM5A – D* transcripts in PHH resulted in similar

203 inhibition of HBV replication as knockdown of the well-characterized host restriction factor
204 DDB1; knockdown of *DDB1* in PHH yielded a reduction in HBV RNA (88 %), HBeAg (91 %),
205 and HBsAg (86 %) by Day 13 as expected [34-37] (**Fig 2A – C**). The kinetics of antiviral
206 activity in *KDM5*-depleted PHH, as measured by inhibition of HBeAg levels over time,
207 suggested that antiviral activity was delayed after siRNA treatment with near maximal antiviral
208 activity achieved by Day 10 – 13 post-initiation of siRNA treatment (**Fig 2D**). Together these
209 data suggest that GS-5801 targets KDM5 to cause antiviral activity and that inhibition of all
210 *KDM5* gene products (*KDM5A – D*) is necessary for restricting HBV replication.
211
212 **Fig 2. Knockdown of *KDM5* confers antiviral activity in PHH.** *KDM4* and *KDM5* transcripts
213 were depleted by siRNA either individually (*KDM4A*, *B*, *C*, *D*, or *E*; *KDM5A*, *B*, *C*, or *D*) or
214 simultaneously (*KDM4A – E* pool; *KDM5A – D* pool) in HBV-infected PHH. *DDB1*, the well-
215 characterized HBV host restriction factor, was also depleted by siRNA for comparison. Fourteen
216 days after initiation of siRNA transfection, levels of (A) intracellular HBV RNA, (B) secreted
217 HBeAg, and (C) secreted HBsAg were measured by qRT-PCR or immunoassay, respectively, for
218 each siRNA condition. (D) The kinetics of HBeAg inhibition is shown for *KDM4A – E* pool,
219 *KDM5A – D* pool, and *DDB1* siRNA conditions. Data shown are the average of two biological
220 replicate experiments and error bars represent the standard deviation.
221
222 Biochemical characterization of GS-080 indicates that it exhibits some inhibitory activity against
223 the KDM4 family of histone lysine demethylases (≥ 13-fold selectivity for KDM5A over
224 KDM4A – C). To examine whether inhibition of KDM4 could also contribute to the antiviral
225 effect observed with GS-5801 in PHH, levels of *KDM4* transcripts were knocked down

226 individually (*KDM4A*, *B*, *C*, *D*, or *E*) or simultaneously (*KDM4A – E*) in PHH. siRNA
227 knockdown of *KDM4* transcripts individually or simultaneously (*KDM4A – E*) resulted in 47 –
228 89 % inhibition of *KDM4* transcript levels in PHH (**SI Fig. 2A, C**) with no effect on cell viability
229 as measured by alamarBlue staining (**SI Fig. 2D**). Knockdown of *KDM4A – E* transcripts
230 simultaneously in HBV-infected PHH resulted in mild inhibition of HBV RNA (57 %), HBeAg
231 (61 %), and HBsAg (47 %) by Day 13 after initiation of siRNA treatment (**Fig 2**); however,
232 *KDM4* depletion did not have as great of an effect on HBV replication compared to *DDB1* or
233 *KDM5A – D* depletion.
234
235 **Antiviral activity of GS-5801 exhibits delayed kinetics**
236 To characterize the kinetics as well as duration of GS-5801 antiviral activity in PHH, we
237 examined the inhibition of secreted HBsAg and HBeAg by GS-5801 in HBV-infected PHH over
238 time. PHH from three different donors were treated with GS-5801 by replacing drug-containing
239 cell culture medium every three to four days for 30 – 32 days. Prior to re-treating cells with
240 GS-5801, levels of HBsAg and HBeAg were measured by immunoassay from PHH supernatant.
241 As shown in **Fig 3**, maximal HBsAg and HBeAg inhibition by GS-5801 was achieved by 12 – 17
242 days after initiation of treatment; similar to the antiviral kinetics observed with *KDM5A – D*
243 siRNA treatment (**Fig 2D**). GS-5801 antiviral activity was maintained throughout the
244 experimental time course of 30 – 32 days (**Fig 3**), indicating that treatment of PHH with
245 GS-5801 maintains HBV antigen reduction in vitro.
246
247 **Fig. 3. Antiviral activity of GS-5801 exhibits delayed kinetics.** PHH from three donors (BCD,
248 VUZ, and 8181) were infected with HBV for three days prior to initiation of GS-5801 treatment.

249 PHH were dosed with vehicle or 10 μM GS-5801 every three to four days for a total of 30 – 32
250 days. At the timepoints shown, levels of secreted (A) HBeAg and (B) HBsAg were measured by
251 immunoassay. Data are plotted as the percentage inhibition of HBeAg or HBsAg in GS-5801
252 treated PHH relative to vehicle treated PHH.
253
254 **GS-5801 causes sustained HBV antigen suppression in PHH**
255 To investigate whether continuous treatment with GS-5801 is necessary to achieve a sustained
256 antiviral response in HBV-infected PHH, we treated PHH with a single, two-hour pulse dose of
257 GS-5801 before removing compound. Antiviral activity was monitored over time by measuring
258 the levels of secreted HBeAg and HBsAg. A pulse dose of GS-5801 reduced cell-associated
259 active parent GS-080 exposure in PHH compared to continuous dosing (**SI Fig 3**; a single two-
260 hour pulse dose of GS-5801 resulted in two-fold lower C_{max} and AUC_{last} values compared to
261 continuous dosing). Furthermore, a pulse dose of GS-5801 in HBV-infected PHH from three
262 independent donors was sufficient to confer antiviral activity with similar kinetics to continuous
263 dosing of GS-5801 (**Fig. 3**; **Fig 4A**). Longer time course experiments probing the antiviral
264 activity of GS-5801 demonstrated that inhibition of HBeAg and HBsAg was sustained up to 20
265 days following a pulse dose (**Fig 4B**).
266
267 **Fig. 4. A single dose of GS-5801 confers sustained HBV antiviral activity in PHH.** (A) PHH
268 from three donors (BCD, 7272, and 8181) were infected with HBV for three days prior to
269 initiation of GS-5801 treatment. PHH were treated once for two hours with vehicle or 10 μM
270 GS-5801. Compound was removed by replacing the medium with fresh medium without drug or
271 vehicle. At the timepoints shown, levels of secreted HBeAg and HBsAg were measured by

272 immunoassay for 12 days. Data are shown as the percentage inhibition of HBeAg or HBsAg in
273 GS-5801 treated PHH relative to vehicle treated PHH. (B) PHH from donor BCD were infected
274 with HBV for three days prior to initiation of GS-5801 treatment. PHH were treated once for two
275 hours with vehicle or 10 μM GS-5801. Compound was removed by replacing the medium with
276 fresh medium without drug or vehicle. At the timepoints shown, levels of secreted HBeAg and
277 HBsAg were measured by immunoassay for 24 days. Data are shown as the average percentage.
278
279 **Global H3K4me3:H3 increases correlate with GS-5801 antiviral activity in PHH**
280 It has been demonstrated that inhibition of KDM5 either genetically or pharmacologically
281 increases levels of H3K4me3 on the mammalian genome [24, 27]. Therefore, we investigated the
282 relationship between global H3K4me3 changes and antiviral activity in HBV-infected PHH
283 treated with GS-5801. HBV-infected PHH were treated either continuously with GS-5801 every
284 three to four days or once with a two-hour pulse dose of GS-5801and the ratio of the levels of
285 H3K4me3 relative to H3 (H3K4me3:H3) were measured by ELISA along with levels of secreted
286 HBeAg to monitor antiviral activity. Continuous dosing of HBV-infected PHH with GS-5801
287 resulted in increased levels of the global H3K4me3:H3 ratio throughout the experimental time
288 course with an apparent saturation of H3K4me3:H3 (4.8-fold increase compared to vehicle
289 treated PHH) occurring six days after initiation of dosing (PHH received two doses of GS-5801;
290 **Fig 5A**). In contrast, a single pulse dose of GS-5801 resulted in a 2.8-fold increase in
291 H3K4me3:H3 by day three that decreased to near baseline levels by day nine (**Fig 5B**).
292 Furthermore, increases in H3K4me3:H3 measured at day three positively correlated with the
293 percentage inhibition of HBeAg measured on day 12 after PHH were treated with a pulse dose of
294 GS-5801 at increasing concentrations (0.016 – 10 μM; **Fig 5C**). Thus, increases in H3K4me3:H3
295 after a pulse dose of GS-5801 precedes the maximal antiviral response. The kinetics of antiviral

296 activity, as assessed by inhibition of secreted HBeAg over time, was similar between continuous
297 and pulse dosing experiments (**Fig 5A, B**). Quantitative mass spectrometry analysis of histones
298 purified from GS-5801 treated PHH corroborated that GS-5801 predominantly caused an
299 increase in trimethylated H3K4 (H3K4me3) as opposed to dimethyl (H3K4me2) or monomethyl
300 (H3K4me) species in PHH (**Fig 5D**). Together these data suggest that levels of the H3K4me3:H3
301 ratio positively correlate with HBV antiviral activity after GS-5801 treatment and that sustained
302 increases in H3K4me3:H3 are not required for GS-5801 antiviral activity.
303
304 **Fig. 5. GS-5801 causes global increases in H3K4me3:H3 that precede antiviral activity.**
305 PHH were infected with HBV for three days prior to initiation of GS-5801 treatment. (A) PHH
306 were treated with vehicle or 10 μM GS-5801 every three to four days for a total of 14 days
307 (continuous dosing). Data shown are from donor 8130 and are representative of data from
308 continuous dosing experiments. (B) PHH were treated with vehicle or 10 μM GS-5801 once for
309 two hours with vehicle or 10 μM GS-5801 prior to replacing medium with fresh medium without
310 drug or vehicle (pulse dosing). Data shown are the average values from three PHH donors (BCD,
311 8181, 7272) and error bars represent the standard deviation. (A, B) At the timepoints shown,
312 levels of secreted HBeAg were measured by immunoassay and are plotted as the percentage
313 inhibition of HBeAg in GS-5801 treated PHH relative to vehicle treated PHH. In addition, levels
314 of H3K4me3 relative to H3 (H3K4me3:H3) were measured by ELISA in vehicle and GS-5801.
315
316 **GS-5801 alters the expression of viral as well as host transcripts in PHH**
317 Given that GS-5801 increases H3K4me3:H3, which is an epigenetic modification associated
318 with transcriptionally active promoters [18-22], we examined the effect of GS-5801 on host and

319 viral transcriptomes using RNA sequencing (RNA-seq). HBV-infected PHH from three donors
320 were treated with GS-5801 every three to four days for 13 days and total cellular mRNA was
321 isolated and sequenced on days 1, 3, 10, and 13 after initiation of dosing. Corroborating our
322 qRT-PCR data (see **Table 2**), levels of HBV mRNA as measured by RNAseq were decreased
323 after GS-5801 treatment in a dose and time dependent manner (**Fig 6A**). Global analyses of host
324 gene expression changes upon GS-5801 treatment (defined as transcripts up or down regulated
325 by ≥ 4-fold compared to vehicle treated PHH, FDR < 0.05) revealed numerous dose and time
326 dependent effects on host transcripts (**Fig 6B; Supplemental Table 6**), with most GS-5801-
327 regulated genes sustained in their expression pattern over the time course (**Fig 6C**). The majority
328 of genes that changed in response to GS-5801 treatment were upregulated and included genes
329 that spanned pathways such as cytoskeleton remodeling and cell-cell junction organization.
330 However, by 10 days after treatment genes were also observed to be downregulated by GS-5801
331 treatment and included genes involved in pathways such as metabolism and biosynthesis (**S**
332 **Table 6**). Notably, interferon-α-stimulated genes (ISG) [38] showed mild transcriptional
333 regulation by GS-5801, but as a class did not exhibit a strong pattern of differential regulation in
334 response to GS-5801 treatment of PHH (**Fig 6D**).
335

336 **Table 2. Antiviral activity of GS-5801 in HBV-infected PHH**
337

PHH Donor[a]	Hu8181	Hu8130	Hu4167	BCD	Hu7272	Hu276	Hu349
vRNA EC_{50} (μM)	0.16 (1.9)	1.1 (3.2)	0.047 (1.1)	0.034 (3.4)	0.93 (3.7)	0.042 (1.8)	0.43 (1.2)
vDNA EC_{50} (μM)	0.14 (3.7)	1.3[b]	0.11 (3.5)	0.0071 (4.9)	1.1 (5.0)	0.070 (1.2)	0.23 (2.4)
HBsAg EC_{50} (μM)	0.061 (2.4)	1.7 (3.7)	0.24 (2.6)	0.015 (3.3)	5.1 (2.1)	0.15 (1.8)	0.97 (3.5)

HBeAg EC_{50} (μM)	0.11 (2.2)	1.1 (2.3)	0.15 (2.7)	0.014 (19)	0.61 (5.5)	0.10 (2.0)	0.38 (2.4)
CC_{50} (μM)	> 10	> 10	> 10	> 10	> 10	> 10	> 10

338 a Data shown are the geometric mean EC_{50} values and the geometric standard deviation factor from HBV-infected PHH
339 treated every three to four days with GS-5801 for 14 days (n = 3 donor Hu8181, n = 3 donor Hu8130, n = 2 donor Hu4167,
340 n = 2 donor BCD, n = 3 donor Hu7272 , n = 2 Hu276, n = 2 Hu349 experiments).
341 b EC_{50} value represents n = 1.

342 **Fig 6. GS-5801 influences host and viral gene transcription.** PHH from three donors (8130,
343 8181, and 4239) were infected with HBV for three days prior to initiation of GS-5801 treatment.
344 PHH were treated continuously with vehicle, 0.03, 0.3, or 10 μM GS-5801 every three to four
345 days for a total of 13 days. PHH were harvested at 1, 3, 10, and 13 days after initiation of GS-
346 5801 dosing and mRNA was quantified by RNA-seq. (A) The number of sequencing reads
347 mapping to the HBV genome were quantified in all samples (counts per million; cpm) and data
348 are plotted as the percentage inhibition of HBV RNA (vRNA) in GS-5801 treated samples
349 relative to vehicle treated samples at each timepoint. (B) The number of genes differentially up
350 or downregulated (differential by 4-fold $\log_2$; FDR < 0.05) in GS-5801 treated PHH compared to
351 vehicle treated PHH are shown for each timepoint. (C) Shown is a Venn diagram demonstrating
352 the overlap of the identity of genes differentially upregulated (fold change ≥ 4-fold $\log_2$; FDR <
353 0.05) in PHH treated with 10 μM GS-5801 compared to vehicle treated PHH for Day 3 (n = 414
354 genes), Day 10 (n = 1131 genes), and Day13 (n = 1268 genes) after initiation of GS-5801 dosing.
355 (D) Interferon-stimulated genes (ISG) expressed in PHH (n = 279) were examined by
356 hierarchical clustering using an uncentered Pearson correlation. Data are displayed as a heatmap
357 of log2 differential cpm values with red representing genes upregulated in GS-5801 treated PHH
358 and blue representing genes downregulated in GS-5801 treated PHH.
359

360 **GS-5801 is liver-targeted in nonclinical species and preferentially increases H3K4me3:H3**
361 **levels in the liver**

362 As HBV is a liver-tropic virus, our pro-drug strategy sought to not only improve the cell-
363 permeability of GS-080 but also its enrichment in the liver. Liver enrichment of GS-080 could
364 reduce systemic exposure to limit epigenetic alteration of host chromatin in other tissues.
365 GS-5801 was identified as an ethyl ester pro-drug of GS-080 with high liver to plasma area
366 under the curve (AUC) ratios for the active parent GS-080 in cynomolgus monkey (**Fig 7A**; 176-
367 fold GS-080 liver to plasma AUC ratio) and rat (**Fig 7B**; 44-fold GS-080 liver to plasma AUC
368 ratio). To investigate the effect of preferential liver exposure of GS-080 on the
369 pharmacodynamic response in vivo (H3K4me3:H3), we dosed cynomolgus monkeys and rats
370 orally once daily with GS-5801 for seven or five days, respectively, and examined global levels
371 of the H3K4me3:H3 ratio by ELISA in liver, lung, kidney, and PBMCs 24 hours after the last
372 dose of GS-5801. Treatment of monkeys (**Fig 7C**) or rats (**Fig 7D**) with GS-5801 resulted in
373 increased levels of the H3K4me3:H3 ratio in the liver compared to lung, kidney, or PBMCs at
374 most doses tested. Furthermore, no adverse effects were observed in rats or monkeys at the
375 GS-5801 doses tested in these studies. Together these data indicate that GS-5801 is a liver-
376 targeted pro-drug that preferentially causes accumulation of H3K4me3:H3 on total cellular DNA
377 at doses that are well tolerated in vivo.
378

379 **Fig. 7. GS-5801 increases H3K4me3:H3 levels preferentially in liver tissue.** Sprague Dawley
380 rats (A) and cynomolgus monkeys (B) were dosed once with 1 mg/kg or 2.5 mg/kg GS-5801
381 p.o., respectively. Amounts of pro-drug (GS-5801) and active parent (GS-080) were measured by
382 LC-MS in liver tissue and plasma at the timepoints shown. (C) Cynomolgus monkeys were

383 dosed p.o. once daily for seven days with 0.03, 0.1, 0.3, 1, 3, or 10 mg/kg of GS-5801. Twenty
384 four hours after the last dose, amounts of H3K4me3 and H3 were measured by ELISA in liver,
385 kidney, PBMCs, and lung. Data are displayed as the average H3K4me3:H3 ratio of GS-5801
386 treated monkeys relative to vehicle treated monkeys from n = 2 – 3 animals; error bars represent
387 the standard deviation. (D) Sprague Dawley rats were dosed p.o. once daily for five days with
388 0.3, 1, 3, 10, or 30 mg/kg of GS-5801. Twenty four hours after the last dose, amounts of
389 H3K4me3 and H3 were measured by ELISA in liver, kidney, PBMCs, and lung. Data are
390 displayed as the average H3K4me3:H3 ratio of GS-5801 treated rats relative to vehicle treated
391 rats from n = 3 animals; error bars represent the standard deviation. (E – F) Wistar Han rats were
392 dosed p.o. once daily for seven days with 10, 30, or 100 mg/kg of GS-5801 and a subset of rats
393 from each dose group continued into a seven day off-treatment phase. (E) Twenty four hours
394 after the last dose or recovery day, amounts of H3K4me3 and H3 were measured by ELISA in
395 the liver. Data are displayed as the average H3K4me3:H3 ratio of GS-5801-treated rats relative
396 to vehicle treated rats from n = 3 animals during the dosing or recovery phases; error bars
397 represent the standard deviation. (F) Transcript levels in rat liver tissue were quantified by RNA-
398 seq (cpm). The number of genes differentially up or downregulated (differential by 2-fold $\log_2$;
399 FDR < 0.05) in GS-5801-dosed rats compared to vehicle-treated rats are shown during the
400 dosing phase (24 hours after once daily dosing for seven days) and recovery phase (24 hours
401 after seven days off drug; F).
402
403 To examine whether increases in H3K4me3:H3 ratios are reversible, similar to the recovery of
404 H3K4me3:H3 ratios to near baseline levels in PHH after a pulse dose of GS-5801 (see **Fig 5B**),
405 rats were dosed once daily for seven days with 0, 10, 30, or 100 mg/kg GS-5801 and a subset of

406 animals continued for seven days off-treatment (recovery phase). Levels of H3K4me3:H3 in rat
407 liver were evaluated by ELISA after seven days of once daily dosing (dosing phase) as well as
408 after seven days off treatment (recovery phase). H3K4me3 and H3 ELISA measurements
409 demonstrated increases in H3K4me3:H3 after seven days of GS-5801 once daily dosing
410 compared to vehicle-treated animals (4.6- to 5.2-fold increase; **Fig 7E**) that agreed with
411 H3K4me3:H3 increases previously observed when rats were dosed once daily for five days with
412 10 or 30 mg/kg GS-5801 (4.2- to 4.3-fold; see **Fig 7D**). When rats were taken off treatment for
413 seven days, H3K4me3:H3 ratio levels returned to near vehicle levels in the 10 and 30 mg/kg
414 dose groups (≤ 1.6-fold of vehicle animals; **Fig 7E**); however, H3K4me3:H3 ratio levels in the
415 100 mg/kg dose group were still elevated above vehicle (2.7-fold increase compared to vehicle
416 treated animals; **Fig 7E**). Next, we examined whether there were any corresponding changes in
417 transcript expression levels that paralleled H3K4me3:H3 increases in GS-5801 treated rats after
418 seven days of once daily treatment as well as after seven days off treatment. Total mRNA from
419 liver tissue of rats dosed for seven days with GS-5801 (0, 10, 30, or 100 mg/kg GS-5801) as well
420 as rats taken off drug for seven days was sequenced with RNA-seq. The number of differentially
421 expressed transcripts were similar after seven days of once daily GS-5801 dosing in rat liver
422 among the 10, 30, and 100 mg/kg dose groups with approximately 300 transcripts differentially
423 regulated between GS-5801 treated groups and vehicle treated (≥ 2-fold differentially regulated,
424 FDR < 0.05; **Fig 7F**). The recovery of H3K4me3:H3 ratios in GS-5801 treated animals to
425 H3K4me3:H3 ratios in vehicle treated animals after seven days off treatment (see **Fig 7E**)
426 corresponded to a return of transcript levels to near vehicle treated levels (**Fig 7F**).
427
428 **GS-5801 is not efficacious in a humanized mouse model of HBV infection**
429

430 To determine whether the antiviral activity of GS-5801 we observed in PHH translated to
431 antiviral efficacy in a nonclinical model, we infected urokinase-type plasminogen activator
432 (uPA) severe combined immunodeficiency (SCID) mice with humanized livers [39] with HBV
433 (genotype C, GTC). HBV infected mice were dosed with 30 or 100 mg/kg of GS-5801. These
434 doses were selected to cause increases in liver H3K4me3:H3 ratios that were comparable to
435 those seen in the PHH infection model that were associated with HBV antiviral activity. Since
436 GS-5801 demonstrated increased levels of H3K4me3:H3 ratios in rat and monkey liver tissue
437 that was well-tolerated and reversible after a seven-day recovery period (see **Fig 7**), we selected
438 a dosing schedule of once daily oral dosing for one week on treatment (qd x 7d) followed by one
439 week off treatment for a total of 56 days (4 treatment cycles). Every seven days, levels of serum
440 HBV DNA and HBsAg were measured to assess the antiviral activity of GS-5801 in this HBV
441 infection model. Treatment of HBV-infected humanized mice with GS-5801 did not result in
442 changes in the amounts of HBsAg or HBV DNA during any of the dosing cycles or recovery
443 periods (**Fig 8A, B**). At the end of the study (Day 56), we measured H3K4me3 and H3 levels in
444 mouse liver tissue by ELISA and observed 2.9- and 3.3-fold increases in H3K4me3:H3 ratios in
445 mice dosed with 30 or 100 mg/kg of GS-5801, respectively, compared to vehicle-treated animals.
446 The increase in H3K4me3:H3 ratios in mouse livers corresponded to an increase in
447 H3K4me3:H3 that was expected to result in antiviral activity for GS-5801 as was observed in the
448 PHH infection model (see **Fig. 5**). Furthermore, the antiviral activity of GS-5801 was assessed in
449 vitro using the primary human hepatocytes that reconstituted the uPA-SCID mouse livers and the
450 HBV GTC virus used in the murine efficacy model. Treatment of these GTC HBV-infected
451 hepatocytes in vitro with GS-5801 every 3 – 4 days resulted in a reduction of HBsAg and

452 HBeAg levels (**Fig. 8D**) similar to what was observed previously with multiple PHH donors and
453 HBV viruses (see **Fig. 5, Table 2, and Table 3**).
454
455 **Fig. 8. GS-5801 does not reduce HBV DNA or HBsAg levels in a humanized mouse model**
456 **of HBV infection.** uPA-SCID mice with humanized livers were infected with HBV GTC virus
457 and dosed p.o. with 30 or 100 mg/kg of GS-5801once daily for seven days in a one week on one
458 week off dosing regimen. Every seven days, levels of HBV DNA (A) and HBsAg (B) were
459 measured. Data is plotted as the average of n = 6 – 8 mice/timepoint/dose group, error bars
460 represent the standard deviation. Shaded grey areas indicate the dosing periods. (C) At study
461 endpoint, Day 56, levels of H3K4me3 and H3 were measured in liver tissue via ELISA to assess
462 GS-5801 pharmacodynamics. Data is shown as the average fold change in H3K4me3:H3 ratio in
463 mice (n = 6 – 8 per dose group) treated with 30 mg/kg or 100 mg/kg of GS-5801 and normalized
464 to vehicle-treated animals; error bars represent the standard deviation. (D) The antiviral activity
465 of GS-5801 was assessed in vitro with the same hepatocytes and GTC virus used in the in vivo
466 HBV efficacy model. Hepatocytes were plated and infected with HBV prior to GS-5801
467 compound treatment. At Day 21, antiviral activity was assessed by measuring extracellular levels
468 of HBsAg and HBeAg. Data is plotted as the average of biological duplicate samples; error bars
469 represent the standard deviation.

470 **Table 3. Antiviral activity of GS-5801 across HBV genotypes**

EC_{50} (µM)[a]	GTA	GTC	GTD	GTE
vRNA	1.8 (1.7)	0.051 (1.7)	0.43 (1.5)	2.7 (3.2)
vDNA	0.17 (2.2)	0.079 (2.0)	0.22 (1.6)	0.25 (7.1)
HBsAg	0.036 (1.0)	0.12 (10)	0.22 (1.0)	3.1 (17)
HBeAg	1.1 (1.5)	N/A[b]	0.30 (1.1)	1.4 (2.4)

471 a Data shown are the geometric mean EC_{50} values and the geometric standard deviation factor from PHH infected with the
472 indicated HBV genotype and treated every three to four days with GS-5801 for 13 days (n = 2 experiments).
473 b Data not available; HBeAg levels were below limit of quantitation by immunoassay.

474

475

476 ## Discussion

477 GS-5801 is an ethyl ester prodrug that metabolizes to GS-080, a potent and selective inhibitor of
478 KDM5a-d. KDM5 enzymes are epigenetic modifiers that demethylate lysine 4 of histone 3 in
479 nucleosomes to regulate gene transcription [14, 15]. In a PHH model of HBV infection, GS-5801
480 demonstrates antiviral activity across multiple HBV genotypes by reducing HBV RNA, DNA,
481 and antigen levels without altering amounts of cccDNA, the transcriptional template of HBV.
482 Knockdown of *KDM5* mRNA levels with siRNA cause a decrease in HBV RNA, DNA, and
483 antigen levels, which further corroborated the role of KDM5 in HBV replication. GS-5801
484 causes a sustained reduction in HBV replication in PHH that correlates with increases in global
485 cellular H3K4me3:H3 levels. Transient increases in H3K4me3:H3 are sufficient for GS-5801
486 antiviral activity in HBV-infected PHH, suggesting that an in vivo dosing strategy of finite
487 treatment periods could be efficacious.

488

489 Detailed in vivo characterization of GS-5801 pharmacokinetic and pharmacodynamic properties
490 (H3K4me3:H3 ratio) reveal that GS-5801 loads the liver with active drug (GS-080) in both
491 nonclinical species examined: rat and cynomolgus monkey (44- and 176-fold liver to plasma
492 AUC ratio, respectively). The enhanced liver levels of GS-080 in rats and cynomolgus monkeys
493 correlates with higher H3K4me3:H3 ratios in the liver compared to other cells and tissues
494 (PBMC, lung, or kidney). Since HBV is a liver-tropic virus that infects hepatocytes, enhancing
495 the distribution of GS-080 to the liver could provide a wider therapeutic index.

496

497 Utilizing knowledge gained from our rat and monkey pharmacokinetic and pharmacodynamic in
498 vivo models as well as our in vitro PHH infection model, we evaluated the antiviral activity of
499 GS-5801 in a humanized mouse model of HBV infection. To our surprise, GS-5801 did not have
500 antiviral activity at either dose tested (30 mg/kg and 100 mg/kg) in the humanized model of
501 HBV infection despite causing H3K4me3:H3 ratios similar to those seen in PHH (2.9- and 3.3-
502 fold increases) based on our in vitro PHH HBV infection data. The reason for the disconnect in
503 GS-5801 antiviral activity in vivo and in vitro is unclear but indicates that increases in
504 H3K4me3:H3 ratio in the liver of HBV-infected humanized mice do not predict antiviral activity
505 as was seen for GS-5801 in the PHH model. Thus, the simple PD marker for KDM5
506 engagement, the H3K4me3:H3 ratio, cannot be considered a straightforward pharamcodynamic
507 marker for GS-5801 antiviral efficacy.
508 Considering how important a new host target for HBV therapy would be, and that the HBV-
509 infected humanized mouse model might not completely predict GS-5801 performance in
510 humans, a small Phase1a/b study was carried out with healthy volunteers and HBV patients

511 (details to be published elsewhere). To our disappointment, GS-5801 was associated with dose
512 limiting, reversible liver toxicity at exposures below reaching significant H3K4me3:H3 ratio
513 increases in patient PBMCs, consistent with the absence of any HBV antigen level decreases (to
514 be published elsewhere), rendering our clinical study inconclusive. Nevertheless, any further
515 clinical evaluation of KMD5 inhibitors in other therapeutic areas should pay close attention to
516 hepatotoxic effects, which might me associated with inhibition of the biologic target even at low
517 levels of engagement.
518
519 Nevertheless, the mechanism by which KDM5 inhibition leads to HBV antiviral activity in PHH
520 remains to be elucidated but should serve to decipher the disconnect between GS-5801 antiviral
521 activity in PHH and the humanized mouse model of HBV infection. Two non-mutually exclusive
522 mechanisms of action for GS-5801 antiviral activity in PHH are hypothesized: (1) modulation of
523 host transcripts by GS-5801 restricts HBV replication indirectly and (2) alteration to the
524 epigenetic landscape of HBV cccDNA reduces HBV transcription directly. As demonstrated by
525 transcriptional profiling of PHH, GS-5801 causes changes in expression levels of many host
526 transcripts and modulation of one or more host transcripts could mediate GS-5801 antiviral
527 activity. Indeed, KDM5 was demonstrated to play a role in respiratory syncytial virus (RSV)
528 pathogenesis as chemical or genetic inhibition of KDM5 in human dendritic cells infected with
529 RSV led to increased transcription of pro-inflammatory cytokines that inhibited RSV replication
530 [40]. In the PHH HBV infection system, the many host transcriptional changes induced by
531 GS-5801 in PHH could make these hepatocytes generally less permissive for HBV replication in
532 vitro. This phenomenon has been proposed for the anti-HBV activity of the retinoid class of
533 compounds which displayed potent antiviral activity in PHH that, however, did not translate in

534 the same humanized mouse model of HBV infection we have employed for GS-5801 [13]. For
535 the retinoid Accutane, its lack of in vivo antiviral activity was hypothesized to be related to
536 differences in transcriptional regulation observed in PHH in vitro versus liver tissue in vivo.
537 Overall, far fewer transcripts were regulated by Accutane in vivo (humanized mouse liver)
538 compared to in vitro (PHH). It was further shown that the culturing process of PHH required to
539 establish permissibility for HBV infection leads to transcriptome changes, many of which were
540 reversed by retinoids [13]. Thus, in vitro transcriptional changes do not always predict in vivo
541 transcriptional regulation. For GS-5801 we observed a similar phenomenon in its in vitro versus
542 in vivo transcriptional regulation, with many fewer host transcripts modulated in liver tissue in
543 vivo (Fig. 7F) compared to PHH in vitro (Fig. 6B), despite achieving similar increases of
544 H3K4me3:H3. It is clear that similar H3K4me3:H3 changes cannot be tied to similar
545 transcriptional responses, thus, rendering our pharmacodynamic marker a poor predictor of
546 GS-5801 in vivo activity.
547
548 Our second hypothesis for GS-5801 antiviral activity in vitro is that inhibition of KDM5 by
549 GS-5801 directly alters the epigenetic landscape of HBV cccDNA to reduce HBV transcription.
550 Although as the consequences of H3K4 trimethylation on cccDNA are not well characterized,
551 activating PTMs (e.g. H3K4me3, H3K27ac) have been associated with HBV transcriptional start
552 sites suggesting that, similar to the host, chromatin modifications contribute to the transcriptional
553 regulation of cccDNA [8-11]. Thus GS-5801 could inhibit HBV transcription by decreasing
554 H3K4me3 levels or changing the spatial organization of H3K4me3 on HBV cccDNA chromatin.
555 This a phenomenon that has been described for some bivalent promoters in eukaryotic cells as
556 the reduction of gene transcription has been correlated with H3K4me3 spread into gene bodies

557 [24]. Alternatively, GS-5801 could also serve to modulate the epigenetic landscape of cccDNA
558 by altering epigenetic modifications that repress transcription of cccDNA (e.g. through
559 H3K27me3 or H3K9me3 that are associated with transcriptionally repressed genes on eukaryotic
560 chromatin) [12, 41].
561
562 In conclusion, this study details nonclinical work characterizing the antiviral activity and
563 pharmacodynamic effects of a small molecule inhibitor of KDM5. GS-5801 demonstrates
564 antiviral activity in a PHH model of HBV infection that correlates with increases in global
565 cellular H3K4me3:H3 ratio, but no antiviral activity is seen in the humanized mouse model of
566 HBV infection despite reaching the desired pharmacodynamic effects expected to be efficacious
567 against HBV. This work highlights the difficulty of epigenetic approaches for therapeutic
568 intervention, especially when the pharmacodynamic effects do not indicate the required
569 engagement of the actual downstream pathogen target(s).
570
571
572

573 ## Materials and Methods

574 **Ethics statement**

575 Primary human hepatocytes (PHH) isolated from deceased donor livers were purchased from
576 Thermo Fisher Scientific (Waltham, MA), Lonza (Basel, Switzerland), BioreclamationIVT
577 (Westbury, NY), and Corning, Inc. (Corning, NY). Consent was obtained from the donor or the
578 donor's legal next of kin for use of the tissue and its derivatives for research purposes using IRB-
579 approved authorizations. Plasma from CHB patients was purchased from Proteogenex (Culver
580 City, CA) or BioCollections Worldwide, Inc (Miami, FL). Consent was obtained from the donor

581 for use of the sample for research purposes using IRB-approved authorizations. All animal work
582 was performed by Covance, Inc. (Princeton, NJ), Crown BioScience, Inc. (Santa Clara, CA) or
583 PhoenixBio Inc. (Higashi-Hiroshima, Japan). Studies in nonclinical species were conducted at
584 test sites fully accredited by the Association for Assessment and Accreditation of Laboratory
585 Animal Care (AAALAC). All procedures in the protocol were in compliance with applicable
586 animal welfare acts and were approved by the local Institutional Animal Care and Use
587 Committees (IACUC) and Animal Ethics Committee. An attending laboratory veterinarian was
588 responsible for providing the medical treatment necessary to prevent unacceptable pain and
589 suffering for the animals on study. All surgery was performed under isoflurane anesthesia, and
590 all efforts were made to minimize suffering.
591 For the clinical studies mentioned above, all patients signed an informed consent form before
592 screening and in accordance with local regulatory and ethics committee requirements. The
593 experimental protocol in these trials was approved by Gilead Sciences and all local regulatory
594 agencies (ANZCTR: **A Phase 1b Study Evaluating the Safety and Tolerability of GS-5801 in Patients**
595 **with Chronic Hepatitis B (ACTRN12616001375448)**)
596

597 **Compounds**

598 GS-5801, GS-080, GS-420 and GS-444 were synthesized by Gilead Sciences, Inc., CanAm
599 Bioresearch, Inc. (Winnipeg, Canada) or by Shanghai Medicilon, Inc. (Shanghai, China). For
600 cell-based assays, compounds were formulated in 100 % DMSO at a concentration of 10 mM.
601 For in vivo studies, GS-5801 was formulated in deionized water.
602

603 **GS-5801 (isolated as the *bis*-tosylate salt):** ^{1}H NMR (400 MHz, Methanol-d_4) δ 8.79 (dd, J = 5.1,
604 0.8 Hz, 1H), 7.95 (s, 1H), 7.90 (dd, J = 5.1, 1.5 Hz, 1H), 7.68 (d, J = 8.2 Hz, 4H), 7.23 (d, J = 7.9
605 Hz, 4H), 4.54 (s, 2H), 4.43 (q, J = 7.1 Hz, 2H), 4.32 (s, 2H), 3.82 (t, J = 5.8 Hz, 2H), 3.46 – 3.34
606 (m, 4H), 2.98 (s, 6H), 2.37 (s, 6H), 1.41 (t, J = 7.1 Hz, 3H), 1.24 (t, J = 7.1 Hz, 3H). LCMS-ESI$^+$
607 (*m/z*): $[M+H]^+$ calcd 337.2; found 337.2.
608
609 **GS-080 (isolated as the *bis*-HCl salt):** ^{1}H NMR (400 MHz, Methanol-d_4) δ 8.78 (dd, J = 5.0, 0.7
610 Hz, 1H), 7.95 (s, 1H), 7.90 (dd, J = 5.0, 1.4 Hz, 1H), 4.52 (s, 2H), 4.25 (s, 2H), 3.81 (t, J = 6.2 Hz,
611 2H), 3.45 – 3.34 (m, 4H), 2.98 (s, 6H), 1.25 (t, J = 7.1 Hz, 3H). LCMS-ESI$^+$ (*m/z*): $[M+H]^+$ calcd
612 309.2; found 309.2.
613
614 **GS-420 (isolated as the *bis*-HCl salt):** ^{1}H NMR (400 MHz, Methanol-d_4) δ 8.92 (d, J = 0.7 Hz,
615 1H), 7.81 (d, J = 0.7 Hz, 1H), 4.52 (s, 2H), 4.45 (q, J = 7.1 Hz, 2H), 4.29 (s, 2H), 3.83 (t, J = 6.0
616 Hz, 2H), 3.47 – 3.36 (m, 4H), 2.98 (s, 6H), 1.41 (t, J = 7.1 Hz, 3H), 1.26 (t, J = 7.1 Hz, 3H).
617 LCMS-ESI$^+$ (*m/z*): $[M+H]^+$ calcd 415.1/417.1; found 415.1/417.1.
618
619 **GS-444 (isolated as the *bis*-HCl salt):** ^{1}H NMR (400 MHz, Methanol-d_4) δ 8.91 (d, J = 0.6 Hz,
620 1H), 7.82 (d, J = 0.7 Hz, 1H), 4.51 (s, 2H), 4.29 (s, 2H), 3.83 (t, J = 6.0 Hz, 2H), 3.40 (dt, J =
621 13.2, 6.5 Hz, 4H), 2.98 (s, 6H), 1.25 (t, J = 7.1 Hz, 3H). LCMS-ESI$^+$ (*m/z*): $[M+H]^+$ calcd
622 387.1/389.1; found 387.1/389.1.
623
624 **PHH plating and culture conditions**
625 Cryopreserved primary human hepatocytes (PHH) isolated from multiple donors were purchased
626 from Thermo Fisher Scientific (HMCPTS; Donors Hu8181, Hu8130, Hu4167, Hu1748,

627 Hu4239), Lonza (HEP187; Donor Hu7272, HUM4167), Bioreclamation (Donors BCD, VUZ), or
628 Corning (Donors Hu276, Hu349, BD195). After thawing, cells were recovered by centrifugation
629 at 100*g* through cryopreserved hepatocyte recovery medium (Thermo Fisher Scientific;
630 CM7500) and plated in collagen coated 96-well plates (Thermo Fisher Scientific; CM1096) at a
631 density of 65,000 – 70,000 live cells per well. Cells were plated in William's E medium (Thermo
632 Fisher Scientific; A1217601) supplemented with 3.6 % hepatocyte thawing and plating
633 supplement (Thermo Fisher Scientific, A15563), 5 % fetal bovine serum (Thermo Fisher
634 Scientific; 16000-036), 1 μM dexamethasone (Thermo Fisher Scientific, A15563), and 0.2 %
635 Torpedo antibiotic mix (Bioreclamation; Z990008). Approximately 12 – 14 hours after plating,
636 plating medium was removed, and cells were switched into maintenance medium: William's E
637 medium supplemented with 4 % hepatocyte maintenance supplement (Thermo Fisher Scientific;
638 AI15564), 2 % fetal bovine serum, 0.1 μM dexamethasone, 1.5 % DMSO (Sigma-Aldrich, St.
639 Louis, MO; D8418), and 0.2 % Torpedo antibiotic mix.

640 **HBV viruses**

641 HepAD38 cells express HBV genotype D (GTD) virions under the control of an inducible
642 tetracycline promoter [42]. For GTD virion production, HepAD38 cells were grown in DMEM-
643 F12 medium (Thermo Fisher Scientific; 11320033) supplemented with 10 % FBS; 1 %
644 Penicillin-Streptomycin-Glutamine; 1 % HEPES, and 1 % non-essential amino acids (Thermo
645 Fisher Scientific). Supernatant containing virions was collected every 3 – 4 days and virions
646 were precipitated with PEGit (Systems Biosciences, Palo Alto, CA; LV810A-1) overnight at
647 4°C. After precipitation, supernatant was spun at 3000 rpm at 4°C for 15 minutes. The pellet
648 containing the virions was resuspended in William's E medium containing 25 % FBS. Viral
649 titers were determined by measuring viral DNA by qPCR.

650

651 For additional HBV genotypes, sera (041FY67821P) from an HBV genotype A (GTA) infected
652 patient and sera (024KY12630) from an HBV genotype E (GTE) infected patient were purchased
653 from Proteogenex. Sera (56662-27867-39729-20130905) from an HBV genotype C (GTC)
654 infected patient was purchased from BioCollections Worldwide, Inc. For the humanized mouse
655 infection model, a GTC virus strain was used that was provided by PhoenixBio (Code No.:
656 PBB004, Lot: 160205).

657

658 **PHH infection with HBV**

659 Approximately 24 hours after plating, PHH were infected with HepAD38-derived GTD virus at
660 500 viral genome equivalents per cell in maintenance medium supplemented with 4 % PEG 8000
661 (Promega, Madison, WI; V3011). For patient sera infections, PHH were infected with 6 µl of
662 patient sera in maintenance medium supplemented with 4 % PEG 8000. Infections were allowed
663 to proceed for 20 – 24 hours before removing remaining extracellular virions by washing with
664 maintenance medium three times.

665

666 **PHH compound treatment**

667 Three days after infection with HBV virus (Day = 0), maintenance medium was replenished, and
668 PHH were dosed in either the continuous or pulse dose regimen with 0, 0.016, 0.037, 0.080,
669 0.11, 0.33, 0.40, 1.0, 2.0, or 10 µM GS-5801 supplied in 100 % DMSO using the HP Digital
670 Dispenser D300 (Hewlett Packard, Palo Alto, CA). For the continuous dose experiment, cells
671 received one dose of GS-5801 on days 0, 3, 6, and 10 and medium was not replenished until the
672 next dose day. For the pulse dose regimen, medium containing compound was removed after two

673 hours incubation and replaced with fresh maintenance medium every three to four days. Cells in
674 the pulse dose experiment received only one dose of compound (Day = 0).
675
676 **Quantitation of extracellular HBV DNA in PHH assays**
677 Viral DNA from PHH supernatants was purified using the Qiagen DNeasy 96 kit (Germantown,
678 MD; 69582) following the manufacturer's recommended protocol. Briefly, 50 µl of supernatant
679 was collected, lysed with an equal volume of Qiagen ATL buffer containing 10 % proteinase K,
680 and then incubated at 56 °C for 10 minutes. Lysates were then mixed with 100 µl of AE buffer
681 containing ethanol, transferred into the DNeasy 96 well plate, and placed onto a vacuum
682 manifold (Qiagen; 19504). The vacuum was applied to bind DNA to the DNeasy membrane
683 while contaminants passed through. DNA bound to the membrane was washed first with 500 µl
684 of AW1followed by 500 µl of AW2 buffer. After washing, plates were centrifuged (Sigma
685 Model 4-16S) at 6000 rpm for 2 minutes. DNA was then eluted with 100 µl of pre-warmed AE
686 buffer by a final centrifugation step of 6000 rpm for 2 minutes.
687 Quantification of vDNA by qPCR (quantitative polymerase chain reaction) amplification of the
688 HBVX region of the genome was performed by combining 5 µl of DNA, 900 nM of forward
689 primer (5'GGA CCC CTG CTC GTG TTA CA 3'), 900 nM of reverse primer (5'GAG AGA
690 AGT CCA CCA CGA GTC TAG A-3'), 0.2 µM TaqMan probe (5' [6FAM] TGT TGA CAA
691 GAA TCC TCA CCA ATA CCA C [NFQ-MGB] 3'), and 1X TaqMan Fast Advanced Master
692 Mix (Thermo Fisher Scientific; 4444557) for a total reaction volume of 20 µl in 96-well PCR
693 plates (Thermo Fisher Scientific; 4346906). qPCR was carried out on a real-time PCR system
694 (Thermo Fisher Scientific; QuantiStudio 7 Flex) using the following conditions: 95 °C for 20

695 seconds, followed by 40 cycles of 95 °C for 1 second and 60 °C for 20 second. A plasmid
696 containing the HBV full genome was used for the standard curve.
697
698 **Quantification of intracellular HBV RNA in PHH assays**
699 Intracellular HBV viral RNA was isolated from PHH using the RNeasy 96 kit (Qiagen, 74182)
700 following the manufacturer's recommended protocol. Briefly, 125 µl of Qiagen RLT lysis buffer
701 was added to PHH. The PHH lysate was then thoroughly mixed with 125 µl of 70 % ethanol,
702 transferred into a RNeasy 96 well plate, and placed onto a vacuum manifold (Qiagen; 19504).
703 The plate was washed using RW1 and RPE buffers, followed by centrifugation (Sigma-Aldrich,
704 Model 4-16S) at 6000 rpm for 2 minutes. The RNA was then eluted twice with 60 µl of nuclease
705 free water for a total of 120 µl RNA.
706 After elution, DNase digestion by Turbo DNase (Thermo Fisher Scientific; AM2239) was
707 performed to remove any contaminating DNA. After 30 minutes of DNase treatment at 37 °C,
708 Turbo DNase was inactivated by adding 15 mM of EDTA and heating the reaction to 75 °C for
709 10 minutes in a thermo cycler (Thermo Fisher Scientific; Veriti 96 Well Thermal Cycler).
710 Quantification of vRNA by qRT-PCR (quantitative reverse transcription polymerase chain
711 reaction) amplification of the HBVX region of the genome was performed by combining 5 µl of
712 RNA to 900 nM of HBVX forward primer (5' GGA CCC CTG CTC GTG TTA CA 3'), 900 nM
713 of HBVX reverse primer (5' GAG AGA AGT CCA CCA CGA GTC TAG A 3'), 0.2 µM
714 TaqMan probe (5' [6FAM] TGT TGA CAA GAA TCC TCA CCA ATA CCA C [NFQ-MGB]
715 3'), and 1X glyceraldehyde 3-phosphate dehydrogenase (GAPDH) or ribosomal protein large P0
716 (RPLP0) endogenous transcripts (Thermo Fisher Scientific; 4310884E; 4310879E) and 1X
717 TaqMan Fast Virus 1-Step Master Mix (Thermo Fisher Scientific; 4444434) for a total reaction

718 volume of 20 µl in 96-well PCR plates (Thermo Fisher Scientific; 4346906). qRT-PCR was
719 carried out on a real-time PCR system (Thermo Fisher Scientific; QuantiStudio 7 Flex) using the
720 following conditions: 50 °C for 5 minutes, then 95 °C for 20 seconds, followed by 40 cycles of
721 95 °C for 3 second and 60 °C for 30 second.
722
723 *GAPDH* or *RPLP0* mRNA expression was used to normalize target gene expression. Levels of
724 HBV RNA for all donors were calculated as fold change relative to no drug treated sample using
725 the 2-ΔΔCt method [43].
726
727 **HBeAg and HBsAg quantification in PHH assays**
728 Hepatitis B e antigen (HBeAg) and Hepatitis B surface antigen (HBsAg) were detected in culture
729 media at the indicated time by ELISA or electrochemiluminescence assay (MSD). The HBeAg
730 and HBsAg ELISAs were performed using the HBeAg ELISA kit (International Immuno-
731 Diagnostics, Foster City, CA) and HBsAg ETI-MAK-2 plus kit (DiaSorin, Stillwater, MN),
732 respectively according to the manufacturer's instructions. Concentrations were calculated by
733 interpolation from standard curves with purified HBeAg and HBsAg. The MSD assay was
734 performed according to the manufacturer's instructions (Meso Scale Diagnostics, Rockville,
735 MD). Briefly, cultured supernatants were inactivated with 0.5% Triton X-100 (30 minutes at
736 37°C) and then transferred into plates pre-spotted with both an anti-HBeAg antibody (Genway
737 Bio, San Diego, CA) and a custom anti-HBsAg antibody. The plates were then incubated for two
738 hours at room temperature with gentle shaking, followed by a wash step in PBS with 0.5%
739 Tween. MSD sulfate tags anti-A and anti-B (1 µg/mL each) were then added to the wells and the
740 plates incubated for a further two hours at room temperature with gentle shaking, followed by

741 another wash step in PBS with 0.5% Tween. A 2X solution of MSD T Buffer Read was then
742 added and the plate was read on a Sector Imager 6000 plate scanner.
743
744 **EC_{50} determination**
745 Antiviral activity of test compounds was determined from vRNA, vDNA, HBeAg, and HBsAg
746 data by comparing compound-treated PHH to DMSO (vehicle)-treated PHH to generate a
747 percent of DMSO control value (% DMSO control). The % DMSO control was calculated by the
748 following equation:
749 % DMSO Control = 100 x (Xc / X_D)
750 where Xc is the signal from the compound-treated PHH and X_D is the signal from the DMSO-
751 treated PHH. The % DMSO control for vRNA, vDNA, HBeAg, HBsAg, *GAPDH*, or *RPLP0* was
752 plotted versus the log of each compound concentration in GraphPad Prism (version 6; Graphpad
753 Software, LaJolla, CA) to generate dose-response curves. EC_{50} values were defined as the test
754 compound concentration that caused a 50% decrease in vRNA, vDNA, HBeAg, or HBsAg. CC_{50}
755 values were defined as the test compound concentration that caused a 50% decrease in *GAPDH*
756 or *RPLP0*. Dose-response curves were fitted using the nonlinear regression equation
757 "log(agonist) versus response – variable slope (four parameters)" in GraphPad Prism to
758 determine EC_{50} values.
759
760 ***KDM4*/*KDM5* siRNA knockdown**
761 PHH from donor HUM4167 were plated in 96-well collagen coated plates at a cell density of
762 65,000 live cells per well as described above and PHH were infected with HepAD38-derived
763 GTD HBV virions at 500 GE per cell. Three days after infection (Day 0) and nine days after

764 infection (Day 6), PHH were transfected with siRNAs targeting *KDM5* or *KDM4* transcripts
765 using Lipofectamine RNAiMAX (Thermo Fisher; 13778150) at a ratio of 6 pmol of siRNA to 1
766 µl RNAiMAX in OptiMEM media (Life Technology; 31985070). 30 µl of siRNA/RNAiMAX
767 complexes were added to appropriate wells containing 150 µl of maintenance medium such that
768 the final concentration of each individual siRNA was 2.5 nM. Three to four siRNAs were used
769 per *KDM5* or *KDM4* gene to insure knockdown of all isoforms. A pool of 14 siRNAs was used
770 to target transcripts of the *KDM5* family (Thermo Fisher 4392420; siRNA: s11834, s11835,
771 s11836, s21144, s21145, s21146, s15748, s15749, s15750, s15775, s15776, s224895, s224896
772 and a custom *KDM5B* siRNA with sense sequence of 5'- ACUUAUUCCUGUCCGGAGAtt -3'
773 and anti-sense sequence of 5'- UCUCCGGACAGGAAUAAGUtg -3'). A pool of 16 siRNAs
774 was used to target the transcripts of the *KDM4* family (Thermo Fisher 4392420; siRNA: s18635,
775 s18636, s18637, s229325, s229326, s22867, s225929, s229931, s225930, s22990, s31266,
776 s31267, s31268, s52751, s52752, s52753). Media was replenished with PHH maintenance
777 media on days 3, 6, 7, and 10 post-initiation of siRNA transfection. On Day 0, 3, 6, 10, and 13
778 post-initiation of siRNA transfection, amounts of secreted HBeAg and HBsAg were measured to
779 assess antiviral activity as described. In addition, on Day 13 alamarBlue (Thermo Fisher;
780 DAL1100) was used as per the manufacturer's protocol to assess toxicity. Intracellular HBV
781 RNA and *KDM* transcripts levels were measured by qRT-PCR to assess antiviral activity and
782 siRNA knockdown. *KDM* primer/probe sets used for qRT-PCR were from Thermo Fisher
783 (4392420): Hs00231908_m1, Hs00981910_m1, Hs01011846_m1, Hs00190491_m1,
784 Hs00206360_m1, Hs00392119_m1, Hs00323906_m1, Hs00250616_s1, Hs00988859_s1, and
785 Hs01096550_m1.
786

787 **cccDNA enrichment and Southern blotting**

788 PHH were plated in 24-well plates at 350,000 – 400,000 live cells per well and infected with
789 HBV genotype D as described above. PHH were treated with GS-5801 every three to four days
790 for 14 days prior to DNA isolation. DNA was isolated from PHH using a MasterPure Complete
791 DNA Purification kit (Epicentre, Madison, WI; MC85200) according to the manufacturer's
792 instructions, but omitting ProteinaseK or RNaseA treatment. After isolation, DNA was treated
793 with T5 exonuclease (New England Biolabs, Ipswich, MA; M0363S) according to the
794 manufacturer's instructions.

795 cccDNA and host mitochondrial DNA (ND4) levels were examined by Southern blot using
796 branched DNA signal amplification (bDNA) method as previously described [44]. All probes
797 and reagents were purchased from Thermo Fisher Scientific.

798 **Rat and cynomolgus monkey in vivo studies**

799 *Liver to plasma GS-5801 and GS-080 AUC ratios*

800 The in vivo portion of the study for determination of liver to plasma drug loading ratios was
801 performed in male Sprague Dawley rats and male cynomolgus monkeys at Covance (Madison,
802 WI). Rats and monkeys were dosed by oral gavage once with 1 mg/kg or 2.5 mg/kg,
803 respectively. The rat study included a vehicle control group (water). Serial venous blood
804 samples were taken at 0, 0.25, 0.5, 1, 2, 4, 6, 8, 12, and 24 hours post dose from each animal and
805 collected into vacutainer tubes containing potassium oxalate/sodium fluoride (Thermo Fisher;
806 BD367925) as the anti-coagulant and blood was centrifuged for plasma isolation. For rat, livers
807 were perfused with heparinized saline sodium nitrite solution immediately prior to harvest and
808 liver samples were excised from vehicle and GS-5801 treated rats at sacrifice at 1, 8, and 24
809 hours post dose (n = 3 per time point). For monkey, liver samples were taken by biopsy at pre-

810 dose, 1, 4, 24, 48, and 72 hours post dose (n = 2 per time point). Rat and monkey livers were
811 weighed and immediately flash frozen in liquid nitrogen.
812
813 500 µL of cold HPLC grade water was added to each monkey liver biopsy sample and rat liver
814 samples were diluted 3-fold with cold HPLC grade water. Diluted liver samples were
815 homogenized between 1 and 3 minutes. 50 µL of plasma samples and homogenized liver samples
816 were quenched with 200 µL of 0.05% formic acid in acetonitrile. Samples were then vortexed
817 and centrifuged at 1500 – 3000 RPM for 15 minutes at RT and diluted as needed with HPLC
818 grade water prior to quantification of GS-5801 and GS-080 by LC-MS/MS. An Agilent 1200
819 series binary pump (Santa Clara, CA; G1312A) was used for elution and separation of
820 compounds with a Hypersil Gold C18 HPLC column (Thermo Fisher; 50 x 3.0 mm, 5 µm) over
821 6.75 minutes with 99 – 3 % gradient of Mobile Phase A (1 % acetonitrile in 2.5 mM ammonium
822 formate aqueous solution pH 2.6) and 1 – 97 % gradient Mobile Phase B (90% acetonitrile in
823 aqueous 10 mM ammonium formate pH 6.8). GS-5801 and GS-080 were detected with a TSQ
824 Quantum Ultra triple quadrupole mass spectrometer in selective reaction monitoring operation
825 mode.
826
827 *Rat and monkey tissue PD (H3K4me3:H3)*
828 The in vivo portion of the study for measurement of tissue PD (H3K4me3:H3 levels) was
829 performed in male Sprague Dawley rats and male cynomolgus monkeys at Crown Bioscience
830 (Taicang, China) and Covance (Madison, WI). Male Sprague-Dawley rats (n = 3 animals per
831 dose group) were dosed p.o. with GS-5801 once daily for five days at 0.3, 1, 3, 10, or 30 mg/kg.
832 Male cynomolgus monkeys (n = 2 or 3 animals per dose group) were dosed p.o. with GS-5801

833 once daily for seven days at 0.03, 0.1, 0.3, 1, 3, or 10 mg/kg. Animals were sacrificed 24 hours
834 post final dose and approximately 100 mg of liver (left lateral lobe), lung, and kidney tissue was
835 collected. Additionally, one mL of venous blood for PBMC isolation was collected into
836 K_2EDTA vacutainer tubes (Thermo Fisher; BD367835). PBMCs were isolated from whole blood
837 that was diluted with an equal volume of Dulbecco's Phosphate Buffered Saline without calcium
838 or magnesium (DPBS; Lonza; 17-512F). Diluted whole blood was layered onto an equal volume
839 of HISTOPAQUE-1077 (Sigma; 10771) gradient medium and centrifuged at 400 x g for 30
840 minutes with the centrifuge brake switch off. PBMCs were collected at the plasma-
841 HISTOPAQUE-1077 interface and washed three times with DPBS by centrifugation at 500 x g
842 for 10 minutes. Tissue samples and PBMCs were snap frozen using liquid nitrogen and stored at
843 -80 °C for subsequent H3K4me3:H3 analysis by ELISA.
844
845 **Evaluation of Tissue Specific PK/PD Response in Cynomolgus Monkeys Dosed with GS-**
846 **5801**
847 Test Site: Crown Biosciences, Taicang, China
848 0.03, 0.1, 0.3 and 1.0 mg/kg/day: 2 males per group
849 **Housing Conditions:** The enrolled monkeys are housed and maintained in accordance with the
850 guidelines approved by the Association for Assessment and Accreditation of Laboratory Animal
851 Care (AAALAC). The targeted conditions for animal living environment and photoperiod are as
852 follows: Temperature: 23 ± 3°C Humidity: 50 ± 20% Light cycle: 12 hours light on and 12 hours
853 light off.

854 **Diet and Enrichment:** All animals have free access to water and are fed twice daily with a
855 complete, nutritionally balanced diet (Beijing Keao Xieli Feed Co., LTD, Beijing, China)
856 enriched with seasonal fruits or vegetables.
857 **Steps to Alleviate Suffering and Clinical Observations**: Non-human primate care and use are
858 conducted in accordance with all applicable assessment and accreditation of laboratory animal
859 care (AAALAC) regulations and guidelines. Crown bioscience institutional animal care and use
860 committee (IACUC) will approve all animal procedures used in this study. All the procedures
861 related to handling, care and treatment of the animals in this study will be performed according
862 to the guidelines approved by the association for AAALAC. After each treatment (weighing,
863 bleeding or dosing), the animals will be observed until the animals are able to stand up and alert
864 if they are anesthetized. At the time of routine monitoring, the animals will be checked for any
865 effects of the compound on their behaviors such as mobility, body weight gain/loss, and any
866 other abnormal activities. Clinical abnormalities observed and animal death will be recorded and
867 reported timely to the veterinarian, study director, and sponsor. Animals will be closely
868 monitored for any abnormal behavior, particularly vomiting, yawning, gaping, and signs of
869 malaise or discomfort.
870 **Anesthesia and Euthanasia:** Animals were humanely euthanized at the end of the study. Those
871 animals were injected with ketamine (15 mg/kg) plus xylazine (2 mg/kg) intramuscularly for
872 anesthesia and operation at the times being sacrificed for tissue collection.
873
874 *Rat liver RNAseq study*
875 The in vivo portion of the study for measurement of rat liver transcript levels by RNAseq was
876 performed at Covance (Madison, WI). Male Wistar Han rats (n = 3 per dose group) were dosed

877 p.o. once daily for seven days with GS-5801 at 10, 30, or 100 mg/kg and sacrificed 24 hours
878 after the last dose. A second group of male Wistar Han rats (n = 3 per dose group) were dosed
879 p.o. once daily for seven days with GS-5801 at 10, 30, or 100 mg/kg and taken off drug for seven
880 days before animals were sacrificed. At sacrifice, two approximately 100 mg samples of liver
881 tissue (left lateral lobe) were collected, snap frozen using liquid nitrogen, and stored at -80 °C for
882 subsequent H3K4me3:H3 analysis by ELISA and transcriptome analysis by RNAseq.
883

884 **HBV mouse efficacy model**

885 The in vivo and in vitro hepatocyte infection model portions of the study were performed by
886 PhoenixBio (Higashi-Hiroshima, Japan). Mice used in this efficacy model (cDNA-
887 uPAwild/+/SCID [cDNA-uPAwild/+: B6;129SvEv-Plau, SCID: C.B-17/Icr-*scid* /*scid* Jcl]) had
888 an estimated human hepatocyte replacement index of 70% or more (PHH# BD195, Corning),
889 which was calculated based on the blood concentration of human albumin prior to the
890 inoculation as previously described [45]. Mice were infected with HBV GTC virus (PhoenixBio;
891 PBB004, Lot #160205) and had serum HBV titer levels greater than 1.0E+08 copies/mL seven
892 days prior to study initiation. HBV-infected mice were treated once daily (p.o.) for seven days
893 (Day 0 – 6) with deionized water for acclimation. Mice (n = 8 per treatment group) received
894 vehicle (deionized water), 30 mg/kg, or 100 mg/kg of GS-5801 p.o. once daily on Days 7 to 13,
895 Days 21 to 27, Days 35 to 41, and Days 49 to 55. Fifty µL of blood was collected from animals
896 under isoflurane anesthesia via the retro-orbital plexus/sinus and centrifuged for serum collection
897 for HBsAg and HBV DNA measurements described below. At termination of study (Day 56),
898 100 – 200 mg of tissue was harvested from the left lateral liver lobe of all animals. Liver tissue

899 samples were snap frozen using liquid nitrogen and stored at -80 °C for subsequent
900 H3K4me3:H3 analysis by ELISA.
901
902 **7-day Oral Gavage Dose Range-Finding Toxicity and Toxicokinetic Study of GS-5801 in**
903 **Male Cynomolgus Monkeys with a 7-day Recovery Phase**
904 Test Site: Covance Laboratories, Madison, WI
905 0, 1, 3, and 10 mg/kg/day: 3 males per group
906 3 additional males at 0 and 3 mg/kg/day for recovery
907 **Housing Conditions**: Animals were housed in stainless steel cages. When possible, animals
908 were socially housed by sex: up to three animals/cage. Animals may be individually housed
909 during acclimation, for study-related procedures, or for behavior or health reasons.
910 Environmental controls for the animal room were set to maintain 20 to 26°C, a relative humidity
911 of 30 to 70%, a minimum of 10 air changes/hour, and a 12-hour light/12-hour dark cycle. The
912 light/dark cycle may be interrupted for study-related activities.
913 **Diet:** Certified Primate Diet #2055C (Envigo RMS, Inc.) was provided one or two times daily
914 unless otherwise specified. The diet is routinely analyzed by the manufacturer for nutritional
915 components and environmental contaminants. Results of specified nutrient and contaminant
916 analyses are on file at Covance-Madison. Water was provided ad libitum. Water samples are
917 routinely analyzed for specified microorganisms and
918 environmental contaminants. The results are on file at Covance-Madison.
919 **Environmental Enrichment:** Animals were given various cage-enrichment devices; fruit,
920 vegetable, or dietary enrichment (that do not require analyses). Animals may or may not be

921 commingled as a form of environmental enrichment due to the limited time for the establishment
922 of compatible pairs (study duration 2 weeks or less).
923 **Steps to Alleviate Suffering**: In accordance with the Animal Welfare Act, the Guide for the
924 Care and Use of Laboratory Animals, and the Office of Laboratory Animal Welfare, medical
925 treatment necessary to prevent unacceptable pain and suffering, including euthanasia, was the
926 sole responsibility of the attending laboratory animal veterinarian. Palliative and prophylactic
927 procedures may be based upon consensus agreement between the Study Director and attending
928 laboratory animal veterinarian. The Study Director and Sponsor/designee (if possible) will be
929 included in discussions of palliative and prophylactic procedures (nonlife-threatening conditions,
930 including suspension of dosing and removal of animals from study) recommended by the
931 attending veterinarian. Final authority for decision making will be with the laboratory animal
932 veterinarian.
933 **Clinical Observations**: Twice daily general observations. One daily cageside observations.
934 Weekly detailed observations. Abnormal findings or an indication of normal was recorded.
935 **Anesthesia and Euthanasia**: Animals were humanely anesthetized at the end of the study with
936 sodium pentobarbital and exsanguinated. Animals may be sedated with ketamine for transport to
937 the necropsy laboratory or for study-related procedures (ie: ECGs).
938
939 *HBsAg measurements from in vivo study*
940 For in vivo mouse studies, serum HBsAg concentrations were determined by SRL, Inc. (Tokyo,
941 Japan) based on the Chemiluminescent Enzyme Immuno Assay (CLEIA) developed by Fujirebio
942 (Lumipulse® Presto II) [46].
943

944 *HBV DNA measurements from in vivo study*

945 HBV DNA was extracted from 5 µL of serum using the SMITEST EX-R&D Nucleic Acid
946 Extraction Kit (Medical & Biological Laboratories, CO. LTD, Nagoya, Japan) and dissolved in
947 20 µL nuclease-free water (Thermo Fisher Scientific Inc., Waltham, MA). Real-time PCR was
948 used to measure the serum HBV DNA concentration using the TaqMan Fast Advanced Master
949 Mix (Thermo Fisher Scientific) and ABI Prism 7500 sequence detector system (Applied
950 Biosystems). The PCR reaction mixture was added into 5 µL of the extracted DNA. The initial
951 activation of uracil-N-glycosylase at 50°C for 2 minutes was followed by the polymerase
952 activation at 95°C for 20 seconds. Subsequent PCR amplification consisted of 53 cycles of
953 denaturation at 95°C for 3 seconds and annealing and extension at 60°C for 32 seconds per cycle
954 in an ABI 7500 sequence detector. The average serum HBV DNA level was calculated from the
955 values of the two separate wells. Forward primer: CACATCAGGATTCCTAGGACC, Reverse
956 primer: AGGTTGGTGAGTGATTGGAG, Probe: CAGAGTCTAGACTCGTGGTGGACTTC
957

958 *Assessment of GS-5801 antiviral activity in PXB hepatocytes in vitro*

959 Hepatocytes were isolated by two-step collagenase perfusion from PXB mice as described [47].
960 Hepatocytes were resuspended in DMEM medium (Thermo Fisher Scientific) containing 2%
961 FBS (Biosera, Kansas City, MO), 20 mM HEPES (Thermo Fisher Scientific), 44 mN $NaHCO_3$
962 (Wako Chemicals, Richmond, VA), 100 IU/mL penicillin (Thermo Fisher Scientific), and 100
963 ug/mL streptomycin (Thermo Fisher Scientific) and plated at a density of 4 x 10^5 cells/well of a
964 BioCoat Collagen I 24 well plate (Corning). Hepatocytes were infected with HBV virus GTC
965 (PXB Strain PBB004, Lot; 20151109) at 5 genome equivalents per cell in DMEM inoculum
966 medium containing 2% DMSO (Sigma-Aldrich), 4% PEG-8000 (Promega), 2% FBS (Biosera),

967 20 mM HEPES (Thermo Fisher Scientific), 44 mN $NaHCO_3$ (Wako Chemicals), 100 IU/mL
968 penicillin (Thermo Fisher Scientific), and 100 ug/mL streptomycin (Thermo Fisher Scientific),
969 15 µg/mL L-proline (Wako Chemicals), 0.25 µg/mL insulin (Sigma-Aldrich), 50 nM
970 dexamethazone (Sigma-Aldrich), 5 ng/mL epidermal growth factor (Sigma-Aldrich), and 0.1
971 mM L-ascorbic acid 2-phosphate (Wako Chemicals). After 24 hours, infection inoculum was
972 removed, cells were washed once with DMEM + 2% FBS and medium was replaced with
973 inoculum medium without PEG. Three days after infection, cells were treated with vehicle
974 (DMSO) or 5-fold serial dilutions of GS-5801 (10 – 0.016 µM). Medium containing fresh
975 compound was replaced every 3 days for a total of six doses of compound and levels of
976 extracellular HBsAg and HBeAg were measured on Day 21.
977
978 *HBsAg and HBeAg measurements from in vitro hepatocyte study*
979 Quantification of HBsAg and HBeAg levels was performed by SRL Inc. (Tokyo, Japan) based
980 on the Chemiluminescent immunoassay (CLIA) using an ARCHITECT instrument and the
981 ARCHITECT HBsAgQT (Abbott, Japan) and ARCHITECT HBeAgQT (Abbott, Japan) reagents
982 [48].
983
984 **H3K4me3:H3 ELISA**
985 Histone extractions and H3K4me3 and H3 measurements from rat and cynomolgus monkey
986 tissue and PBMCs were performed at Crown Bioscience (Taicang, China).
987 *Histone enrichment*
988 Histones were enriched from tissue and PBMC samples using the AbCam total histone extraction
989 kit (Cambridge, UK; ab113476) according to the manufacturer's protocol after cell/tissue

990 dissociation with an IKA T10 TURRAX homogenizer (Wilmington, NC; EW-04720-50).
991 Histones were enriched from 500,000 to 750,000 PHH. PHH monolayers were washed once with
992 cold (4°C) 1X DPBS (Dulbecco's phosphate buffered saline; 21-031-CV, Corning Inc.). Cold
993 triton extraction buffer (TEB): 1X DPBS, 0.5 % triton X-100 (Sigma-Aldrich, T9284), 2 mM
994 phenylmethylsulfonyl fluoride (PMSF; Thermo Fisher Scientific, 36978), was added to the cell
995 monolayer at a density of 1 x 10^6 cells/mL. After 10-minute incubation in TEB at 4°C, the cell
996 monolayer was scraped and cells were pelleted by centrifuged at 1200 rpm at 4°C for 10
997 minutes. The cell pellets were washed again in TEB by centrifugation at 1200 rpm at 4°C for 10
998 minutes. The resulting cell pellet was re-suspended in cold (4°C) 0.2 Normal hydrochloric acid
999 (HCl; Sigma-Aldrich, 343102) at a density of ~ 1 x 10^7 cells/mL and incubated at 4°C for 30
1000 minutes. After incubation, HCl extractions were pelleted by centrifugation at 1200 rpm for 5
1001 minutes at 4°C and supernatant containing the enriched histones was collected.
1002 Total protein concentration of all samples following histone enrichment was determined using a
1003 bicinchoninic acid (BCA) assay (Thermo Fisher Scientific; 23225).
1004
1005 *H3K4me3:H3 ELISA*
1006 An indirect ELISA assay was used to measure amounts of H3K4me3 relative to total H3
1007 (H3K4me3:H3) extracted from tissue, PBMC, or PHH samples. Amounts of H3, H3K4me3, and
1008 non-specific background from the secondary antibody (blank absorbance) were measured for
1009 each sample in independent ELISA wells. Briefly, each histone extraction from tissue or PBMC
1010 lysates was diluted in 50 mM Na_2CO_3 (Sigma-Aldrich; 223484), pH 9.5 coating buffer and 50 µl
1011 of each diluted sample was added to 384-well plates (Greiner, Kremsmünster, Austria; 781061)
1012 in duplicate. A coating concentration for tissue and PBMC histone extracts was used such that

1013 the H3 and H3K4me3 OD measurements were in the linear range for the H3 and H3K4me3
1014 antibodies. After plates were incubated overnight at 4°C to allow for coating of histone samples,
1015 plates were blocked for one hour at room temperature (RT) in 100 µl 5 % skimmed milk (Fluka;
1016 70166)/1X DPBS (Gibco; 70011-044) % w/v solution. Plates were washed three times with
1017 0.1% Tween-20 (Amresco; 0777)/1 X DPBS % v/v solution (DPBST) and 50 µl/well of 0.05
1018 µg/ml H3 (Sino Biological; 11231-RP02) or 0.5 µg/ml H3K4me3 (Millipore; 07473) primary
1019 antibodies diluted in 1X DPBS were added to the ELISA plates and incubated for one hour at
1020 RT. After primary antibody incubation, plates were washed 3 times with 100 µl/well PBST and
1021 50 µl/well of an AbCam secondary antibody (ab137914) diluted to 0.05 µg/ml in 1X PBS was
1022 added to the ELISA plates and incubated for one hour at RT. Plates were washed five times with
1023 100 µl/well DPBST and 50 µl/well 3,3′,5,5′-tetramethylbenzidine (TMB) substrate solution
1024 (Sigma; T0440) was added to each plate. Upon color development (~ three – five minutes),
1025 reactions were quenched by adding 50 µl/well of 1 M H_2SO_4 (Sigma; 72266). Absorbance of
1026 each well was measured at 450 nm within five minutes using a SpectraMax Plus 384 Microplate
1027 Reader (Molecular Devices; PLUS 384).
1028
1029 **Histone Mass Spectrometry**
1030 *Histone Purification from PHH*
1031 Approximately 25 million PHH from Donor BCD (Bioreclamation) were plated on collagen
1032 coated (Coating Matrix kit, Life Technologies, Cat. #R-011-K) plates (coated for 30 minutes at
1033 37°C and subsequently washed twice with PHH plating medium). The PHH plating medium was
1034 removed after 16 hours and replaced with PHH maintenance medium (Day 0). Fresh
1035 maintenance medium supplemented with DMSO or 10 µM GS-5801 was added 3 days later

1036 (Day 3). The maintenance medium was refreshed again with 10 µM GS-5801 or DMSO control
1037 on Day 6, and the histones were extracted and purified 24 hours later (Day 7) using the Active
1038 Motif histone purification mini kit (Cat. #40026). Modifications to the manufacturer's protocol
1039 included two PBS washes prior to adding the histone extraction buffer to the cells, precipitation
1040 of eluted histones in 8 % perchloric acid, and a single wash in cold acetone containing 0.2 %
1041 HCl.

1042 *Propionic Anhydride Labeling*

1043 3 µg of purified core histones from control and GS-5801 treated PHH were diluted with
1044 deionized H_2O to a total volume of 9 µl and buffered to pH 8.5 by addition of 1 µl of 1 M
1045 triethylammonium bicarbonate buffer. Fresh 1:100 propionic anhydride:water reagent was
1046 prepared and 1 µl of mixture was added immediately to the histone sample with vortexing and
1047 incubated for 5 minutes at 25°C. The reaction was quenched with 1 µl of 80 mM hydroxylamine
1048 for 20 minutes at 25°C. Tryptic digestion was performed overnight with 0.3 µg trypsin (Promega
1049 Sequencing Grade; Madison, WI) per sample. Samples were dried down in a speed vac and
1050 resuspended in 20 µl 0.1 M TEAB. To label the peptide N-termini, fresh 1:100 propionic
1051 anhydride (light) and 1:100 d10-propionic anhydride (heavy) in water were prepared and used to
1052 label the control or GS-5801 treated digests by adding 2 µl and incubating samples for 5 minutes
1053 at 25°C. The reaction was quenched with 1 µl of 80 mM hydroxylamine for 20 minutes at 25°C,
1054 dried down in a speed vac, and the resulting control and treated samples were resuspended and
1055 combined in 50 µl of 3 % ACN and 0.1 % formic acid for analysis by mass spectrometry.

1056 *Mass Spectrometry*

1057 1 µl of sample was injected using a Thermo Fischer Scientific Ultimate 3000 Autosampler (San
1058 Jose, CA) onto a 15 cm x 75 µm Thermo Fischer Scientific ES812 Easyspray nano column with

1059 5 µm particle size. Separation was performed using an Thermo Fischer Scientific Ultimate nano
1060 3000 UHPLC with a 300 nl/min flow rate (solvent A (0.1 % formic acid) and solvent B (90%
1061 acetonitrile, 0.1% formic acid)) with a gradient from 3 % solvent B to 35 % (60 min), then 3 %
1062 to 9 % (15 min), holding at 90 % for 5 min, and finally re-equilibrating for 20 min at 3 % solvent
1063 B. Mass spectrometric analysis was performed using a ThermoFischer Scientific Q-Exactive HF
1064 using a data dependent acquisition. Precursor scans from 350-1200 m/z as performed at 120 K
1065 resolution using 50 ms maximum fill time and 3e6 AGC target. The top 15 ions were selected for
1066 MSMS analysis at 15 K resolution using normalized collision energy of 27 with a 50 ms fill time
1067 and 1E5 AGC target. Each sample was analyzed three times.
1068
1069 *Data Analysis*
1070 Data was searched using Thermo Fischer Scientific Proteome Discoverer V2.1 software. Peak
1071 intensities corresponding to unmodified, methylated, dimethylated, and trimethylated H3K4
1072 peptide "TKQTAR" were manually extracted using ThermoFischer Scientific Xcaliber software.
1073 The ratio of drug treated/control was calculated for each sample and then corrected using the
1074 average protein level ratio to account for differences in total protein between control and treated
1075 samples.
1076
1077 **Biochemical characterization**
1078 *Biochemical reagents*
1079 SI Table 3 contains detailed information about the sources of the recombinant enzymes. Peptide
1080 substrates were from AnaSpec (Fremont, CA). α-Ketoglutarate (disodium salt dihydrate, 75892),
1081 L-ascorbic acid (A0278), ammonium iron (II) sulfate hexahydrate (215406), BSA (A3803), and

1082 β-nicotinamide adenine dinucleotide (NAD, N6522) were from Sigma-Aldrich. Tween-20 (10%,
1083 28320) was from Thermo Fisher Scientific. 384 Alpha-plates, acceptor beads (5 mg/mL), alpha
1084 streptavidin donor beads (5 mg/mL, 6760002), and 5× Epigenetic buffer (AL008) were from
1085 PerkinElmer (Waltham, MA). Chicken core histones were obtained from Millipore (Billerica,
1086 MA). HeLa cell nucleosomes were from Reaction Biology Corporation (Malvern, PA).
1087 Nucleosome antigen was from Arotec Diagnosis (ATN02, Wellington, New Zealand). Small
1088 molecule inhibitors used as positive controls included S2101 (CalBiochem/Millipore; 489477),
1089 2,4-Pyridinedicarboxylic acid (AK Scientific, Union City, CA; 00473), 8-hydroxyquinoline
1090 (Sigma-Aldrich; S018), 8-hydroxy-5-quinolinecarboxylic acid (Sigma-Aldrich; SML0057), S-
1091 (5′-Adenosyl)-L-homocysteine (Sigma-Aldrich; A9384), Trichostatin A (Sigma-Aldrich;
1092 T8552), and EX-527 (Sigma-Aldrich; E7024).
1093 *KDM enzymatic assays*
1094 The following assay protocol was used for all histone demethylases tested except KDM1A,
1095 KDM5A, B, and D, which are described below. Compounds were serially diluted into a 384-well
1096 Alpha plate as a DMSO solution and mixed with 5 μL reaction buffer (buffer A) containing 50
1097 mM HEPES (pH 7.0), 0.1% BSA, and 0.003% Tween-20. The enzyme of interest was pre-
1098 incubated with 15 μM of Fe^{2+} for 10 min (except 30 min for KDM2B) in reaction buffer A. 5 μL
1099 of the enzyme mixture was added to each of the compound-containing wells and incubated for
1100 10 min. The reaction was started by addition of a 5 μL mixture containing 300 nM peptide
1101 substrate, 75 μM L-ascorbic acid, and 30 μM α-ketoglutarate in buffer A. This final 15 μL of
1102 reaction mixture was incubated for 20 min for KDM5B and 1 hour for the other KDM enzymes.
1103 The reaction was quenched with 10 μL of diluted AlphaLISA Acceptor beads (1:400) in
1104 Epigenetics Buffer and incubated for 60 min. The Donor beads were diluted 1:400 into

1105 Epigenetics Buffer in the dark and 10 μL of this was added to each well and incubated for
1106 another 60 min in the dark. The assay plates were read on an Enspire plate reader (PerkinElmer)
1107 using a standard AlphaLISA program.
1108 KDM5A and 5B were tested using CisBio HTRF assay platform by Reaction Biology Corp
1109 (Malvern, PA). All concentrations are final unless noted otherwise. Inhibitors were pre-incubated
1110 with 2.5 nM KDM5A or 1.2 nM KDM5B in a 5 μL reaction mixture containing 50 mM HEPES
1111 (pH 7.5), 50 mM NaCl, 0.01% Tween 20, 0.01% BSA for 15 min temperature. The reaction was
1112 initiated by addition of 5 μL of 50 nM Biotin-H3K4me3 and incubated with gentle shaking for
1113 45 min at RT. The reaction was quenched with 10 mM EDTA and 200 mM potassium fluoride.
1114 Upon addition of Eu-Antibody and Streptavidine-XL665, the mixture was incubated for 2 hours
1115 in the dark. The fluorescence resonance energy transfer was measured using an excitation
1116 wavelength of 320 nm and emission wavelength of 665 nm on an Envision plate reader (Perkin
1117 Elmer).
1118 KDM5D was tested using a LANCE TR-FRET assay by Eurofins Cerep SA (France). All
1119 concentrations were final unless noted otherwise. Inhibitors were added to a mixture containing
1120 45 mM HEPES/Tris-HCl (pH 7.5), 5 μM ferrous ammonium sulfate, 100 μM ascorbic acid, 10
1121 μM 2-oxoglutarate, 0.01% Tween 20, 0.01% BSA, and 10 ng of enzyme, followed by addition of
1122 100 nM biotin-H3K4me3 substrate. The 10 μL reaction mixture was incubated for 10 min at
1123 room temperature and quenched through the addition of 1 mM EDTA to reach a final
1124 concentration of 0.33 mM EDTA. After 5 min, the Eu-labeled anti-methyl histone H3K4me1-2
1125 antibody and the Ulight streptavidin were added, and the mixture was incubated for 60 min. The
1126 fluorescence resonance energy transfer was measured using an excitation wavelength of 320 nm
1127 and emission wavelengths of 620 nm and 665 nm on an Envision plate reader (Perkin Elmer).

1128 The KDM1 assay was conducted in the presence of NAD but without Fe(II) or ascorbic acid. A
1129 10 µL reaction mixture containing 50 mM Tris-HCl (pH 9.0), 50 mM NaCl, 0.01% Tween-20,
1130 0.25 nM of enzyme, and 1 mM NAD was pre-incubated for 10 min. The reaction was started by
1131 addition of 5 µL of H3(1-21)K4 me1, and the reaction mixture was incubated for 60 min. The
1132 reaction was quenched with 10 µL AlphaLISA Acceptor beads (1:200) in Epigenetics Buffer and
1133 the reaction mixture was incubated for 60 min. The Donor beads were diluted 1:200 into
1134 Epigenetics Buffer in the dark, and 10 µL of this mixture was added to each well and incubated
1135 for another 60 min in the dark. The assay plates were read on an Enspire plate reader
1136 (PerkinElmer) using a standard AlphaLISA program.

1137 *Histone methyltransferase enzymatic assays*

1138 Histone methyltransferase assays were performed in 96-well half-area optiplates (PerkinElmer)
1139 at room temperature. All concentrations are final unless noted otherwise. Compounds were
1140 serially diluted in DMSO and the final DMSO concentration was 1%. A 24 µL reaction mixture
1141 contained compound, enzyme, 200 nM of nucleosome or histone substrate, 400 nM ^{3}H-SAM
1142 (83.1 Ci/mmol), 50 mM Tris-HCl (pH 8.0), 50 mM NaCl, 5 mM $MgCl_2$, 1 mM DTT, and 0.01%
1143 Tween-20. The plate was sealed, mixed on a Titramax plate shaker at 1200 rpm for 30 sec, and
1144 incubated at room temperature for 60 min. The reaction was quenched by addition of 24 µL
1145 mixture containing 5 mg/mL PVT-PEI beads and 300 µM unlabeled SAM in water. The plate
1146 was sealed, mixed as previously noted, incubated overnight, and read on a TopCount plate reader
1147 (PerkinElmer).

1148 *Histone deacetylase enzymatic assays*

1149 The HDAC-1 histone deacetylase assay was tested using the FLUOR DE LYS platform (Cisbio,
1150 Bedford, MA). Inhibition of SIRT-1 histone deacetylase was tested with the AlphaLISA

1151 detection system. All assays were conducted at room temperature with a final DMSO
1152 concentration of 1%. The HDAC-1 reactions were started by incubating a 5-μL mixture
1153 containing 50 mM Tris-HCl (pH 8.0), 137 nM NaCl, 2.7 mM KCl, 1 mM $MgCl_2$, 1 mg/mL BSA,
1154 10 nM HDAC-1, and various concentrations of inhibitors for 10 minutes prior to addition of 5
1155 μL 100 μM fluorogenic peptide from p53 residues 379-382 [RHKK(Ac)AMC]. After a 60-120-
1156 minute incubation at 30 ºC, the reaction was quenched with 2 μM trichostatin A (final
1157 concentration), mixed with 10 μL of Developer and incubated at 30 ºC for 1 hr. The fluorescence
1158 signal was measured using an excitation wavelength of 360 nm and emission wavelength of 460
1159 nm on an EnVision Multilabel plate reader (PerkinElmer). The SIRT-1 reactions were carried out
1160 in a 15 μL mixture containing 50 mM Tris-HCl (pH 8.0), 150 nM NaCl, 1 mM DTT, 0.01%
1161 Tween-20, 0.01% BSA, 5 nM enzyme, 1 mM NAD, and 25 nM H3(1-21)K4(Ac) substrate. After
1162 a 60-minute incubation, the reaction was quenched with 10 μL AlphaLISA H3K4-specific
1163 Acceptor beads (1:200) in Epigenetics Buffer, and the reaction mixture was incubated for 60
1164 min. The Donor beads were diluted 1:200 into Epigenetics Buffer in the dark and 10 μL of this
1165 mixture was added to each well and incubated for another 60 min in the dark. The assay plates
1166 were read on an Enspire plate reader (PerkinElmer) using a standard AlphaLISA program.
1167 *IC50 determination*
1168 The IC50 value was defined as the concentration of inhibitor inducing 50% decrease in product
1169 formation. Data was analyzed using GraphPad Prism 6.0 (La Jolla, CA). Unless otherwise
1170 mentioned, IC50 values were calculated by non-linear regression analysis using sigmoidal dose-
1171 response (variable slope) equation (four parameter logistic equation):
1172 Y= Bottom + (Top-Bottom)/(1+10^((LogIC50-X)*HillSlope)),

1173 where X is log of the concentration of the inhibitor, Y is the response, the Bottom and Top
1174 values were fixed at 0% and 100%, respectively. IC50 values were calculated as an average of at
1175 least two independent experiments.
1176

1177 **RNA-Seq library preparation and analysis**

1178 Library building and sequencing for RNA-seq of PHH and rat liver was performed on all
1179 samples at EA Genomics/Q2 Solutions (Morrisville, NC). Approximately 100 mg of rat liver
1180 tissue from the left later lobe was flash frozen immediately after collection. PHH were lysed into
1181 RLT buffer (Qiagen; 79216) and immediately frozen. Liver/PHH samples were homogenized in
1182 QIAzol Lysis Reagent (79306) and after addition of chloroform the samples were separated into
1183 aqueous and organic phases by centrifugation. Ethanol was added to the upper aqueous phase
1184 and the sample was applied to an RNeasy Mini spin column (74104) for purification and RNA
1185 eluted with water. Libraries were prepared using the Illumina TruSeq stranded mRNA sample
1186 preparation kit according to the manufacturer's protocol (Illumina, Inc., Hayward, CA; RS-122-
1187 2103). Approximately 30 million 2 x 50 bp paired-end reads were collected per sample using the
1188 Illumina HiSeq2000 sequencing platform. Sequencing reads were aligned to the human, rat, or
1189 HBV genomes by STAR [49]. The Bioconductor packages edgeR [50] and limma [51] were used
1190 to normalize sequence count data (counts per million; cpm) and conduct differential gene
1191 expression analysis. The false discovery rate (FDR) was calculated using the Benjamini-
1192 Hochberg method [52].
1193

1194 **Data availability**

1195 RNASeq data generated in this study were deposited in the Gene Expression Omnibus
1196 (http://www.ncbi.nlm.nih.gov/geo) with accession numbers GSE166040 and GSE165727.
1197

1198 ## Acknowledgements

1199 Funding for this research was provided by Gilead Sciences, Inc. S.G., D.T., T.C, C.S., J.F.,
1200 M.M., J.Y.F., R.R., L.L., H.Y., Y.X., D.B., T.A., M.W., T.K., U.S., G.N., and B.F. are
1201 employees of Gilead Sciences, Inc. R.D., G.C., K.B., G.B., E.P., C.T., W.D. were previously
1202 employed by Gilead Sciences, Inc. All authors may hold stock or stock options in Gilead
1203 Sciences, Inc.
1204

1205 We thank Gary Lee and Hoa Truong for performing the MSD immunoassay; Lindsay Gamelin
1206 for PHH donor screening as well as assistance identifying patient serum samples, as well as
1207 Tomas Cihlar, Anuj Gaggar, and Vithika Suri for helpful suggestions and discussions.
1208

1209
1210

1211 # References

1212

1213 1. Lozano R, Naghavi M, Foreman K, Lim S, Shibuya K, Aboyans V, et al. Global and regional mortality
1214 from 235 causes of death for 20 age groups in 1990 and 2010: a systematic analysis for the Global Burden of
1215 Disease Study 2010. Lancet. 2012;380(9859):2095-128. Epub 2012/12/19. doi: 10.1016/S0140-6736(12)61728-0.
1216 PubMed PMID: 23245604.
1217 2. Schweitzer A, Horn J, Mikolajczyk RT, Krause G, Ott JJ. Estimations of worldwide prevalence of chronic
1218 hepatitis B virus infection: a systematic review of data published between 1965 and 2013. Lancet. 2015;386:1546-
1219 55. Epub 2015/08/02. doi: 10.1016/S0140-6736(15)61412-X. PubMed PMID: 26231459.
1220 3. World Health Organization. Hepatitis B Fact Sheet2018. p. https://www.who.int/en/news-room/fact-
1221 sheets/detail/hepatitis-b.
1222 4. Kwon H, Lok AS. Hepatitis B therapy. Nat Rev Gastroenterol Hepatol. 2011;8(5):275-84. Epub
1223 2011/03/23. doi: 10.1038/nrgastro.2011.33. PubMed PMID: 21423260.
1224 5. Newbold JE, Xin H, Tencza M, Sherman G, Dean J, Bowden S, et al. The covalently closed duplex form of
1225 the hepadnavirus genome exists in situ as a heterogeneous population of viral minichromosomes. J Virol.
1226 1995;69(6):3350-7. PubMed PMID: 7745682; PubMed Central PMCID: PMCPMC189047.
1227 6. Nassal M. HBV cccDNA: viral persistence reservoir and key obstacle for a cure of chronic hepatitis B. Gut.
1228 2015;64(12):1972-84. doi: 10.1136/gutjnl-2015-309809. PubMed PMID: 26048673.
1229 7. Revill P, Locarnini S. Antiviral strategies to eliminate hepatitis B virus covalently closed circular DNA
1230 (cccDNA). Curr Opin Pharmacol. 2016;30:144-50. doi: 10.1016/j.coph.2016.08.015. PubMed PMID: 27639371.
1231 8. Pollicino T, Belloni L, Raffa G, Pediconi N, Squadrito G, Raimondo G, et al. Hepatitis B virus replication
1232 is regulated by the acetylation status of hepatitis B virus cccDNA-bound H3 and H4 histones. Gastroenterology.
1233 2006;130(3):823-37. Epub 2006/03/15. doi: 10.1053/j.gastro.2006.01.001. PubMed PMID: 16530522.
1234 9. Levrero M, Pollicino T, Petersen J, Belloni L, Raimondo G, Dandri M. Control of cccDNA function in
1235 hepatitis B virus infection. J Hepatol. 2009;51(3):581-92. doi: 10.1016/j.jhep.2009.05.022. PubMed PMID:
1236 19616338.
1237 10. Tropberger P, Mercier A, Robinson M, Zhong W, Ganem DE, Holdorf M. Mapping of histone
1238 modifications in episomal HBV cccDNA uncovers an unusual chromatin organization amenable to epigenetic
1239 manipulation. Proc Natl Acad Sci U S A. 2015;112(42):E5715-24. Epub 2015/10/07. doi:
1240 10.1073/pnas.1518090112. PubMed PMID: 26438841; PubMed Central PMCID: PMC4620859.
1241 11. Palumbo GA, Scisciani C, Pediconi N, Lupacchini L, Alfalate D, Guerrieri F, et al. IL6 Inhibits HBV
1242 Transcription by Targeting the Epigenetic Control of the Nuclear cccDNA Minichromosome. PLoS One.
1243 2015;10(11):e0142599. doi: 10.1371/journal.pone.0142599. PubMed PMID: 26580974; PubMed Central PMCID:
1244 PMCPMC4651563.
1245 12. Allis CD, Jenuwein T. The molecular hallmarks of epigenetic control. Nat Rev Genet. 2016;17(8):487-500.
1246 doi: 10.1038/nrg.2016.59. PubMed PMID: 27346641.
1247 13. Birkus G, Snyder C, Jordan R, Kobayashi T, Dick R, Puscau V, et al. Anti-HBV activity of retinoid drugs
1248 in vitro versus in vivo. Antiviral Res. 2019;169:104538. Epub 2019/06/22. doi: 10.1016/j.antiviral.2019.104538.
1249 PubMed PMID: 31226346.
1250 14. Walport LJ, Hopkinson RJ, Schofield CJ. Mechanisms of human histone and nucleic acid demethylases.
1251 Curr Opin Chem Biol. 2012;16(5-6):525-34. doi: 10.1016/j.cbpa.2012.09.015. PubMed PMID: 23063108.
1252 15. Klose RJ, Kallin EM, Zhang Y. JmjC-domain-containing proteins and histone demethylation. Nat Rev
1253 Genet. 2006;7(9):715-27. doi: 10.1038/nrg1945. PubMed PMID: 16983801.
1254 16. Christensen J, Agger K, Cloos PA, Pasini D, Rose S, Sennels L, et al. RBP2 belongs to a family of
1255 demethylases, specific for tri-and dimethylated lysine 4 on histone 3. Cell. 2007;128(6):1063-76. doi:
1256 10.1016/j.cell.2007.02.003. PubMed PMID: 17320161.
1257 17. Klose RJ, Yan Q, Tothova Z, Yamane K, Erdjument-Bromage H, Tempst P, et al. The retinoblastoma
1258 binding protein RBP2 is an H3K4 demethylase. Cell. 2007;128(5):889-900. doi: 10.1016/j.cell.2007.02.013.
1259 PubMed PMID: 17320163.
1260 18. Lauberth SM, Nakayama T, Wu X, Ferris AL, Tang Z, Hughes SH, et al. H3K4me3 interactions with
1261 TAF3 regulate preinitiation complex assembly and selective gene activation. Cell. 2013;152(5):1021-36. doi:
1262 10.1016/j.cell.2013.01.052. PubMed PMID: 23452851; PubMed Central PMCID: PMCPMC3588593.

1263 19. Heintzman ND, Stuart RK, Hon G, Fu Y, Ching CW, Hawkins RD, et al. Distinct and predictive chromatin
1264 signatures of transcriptional promoters and enhancers in the human genome. Nat Genet. 2007;39(3):311-8. doi:
1265 10.1038/ng1966. PubMed PMID: 17277777.
1266 20. Santos-Rosa H, Schneider R, Bannister AJ, Sherriff J, Bernstein BE, Emre NC, et al. Active genes are tri-
1267 methylated at K4 of histone H3. Nature. 2002;419(6905):407-11. Epub 2002/09/28. doi: 10.1038/nature01080.
1268 PubMed PMID: 12353038.
1269 21. Schneider R, Bannister AJ, Myers FA, Thorne AW, Crane-Robinson C, Kouzarides T. Histone H3 lysine 4
1270 methylation patterns in higher eukaryotic genes. Nat Cell Biol. 2004;6(1):73-7. Epub 2003/12/09. doi:
1271 10.1038/ncb1076. PubMed PMID: 14661024.
1272 22. Vermeulen M, Mulder KW, Denissov S, Pijnappel WW, van Schaik FM, Varier RA, et al. Selective
1273 anchoring of TFIID to nucleosomes by trimethylation of histone H3 lysine 4. Cell. 2007;131(1):58-69. doi:
1274 10.1016/j.cell.2007.08.016. PubMed PMID: 17884155.
1275 23. Ram O, Goren A, Amit I, Shoresh N, Yosef N, Ernst J, et al. Combinatorial patterning of chromatin
1276 regulators uncovered by genome-wide location analysis in human cells. Cell. 2011;147(7):1628-39. doi:
1277 10.1016/j.cell.2011.09.057. PubMed PMID: 22196736; PubMed Central PMCID: PMCPMC3312319.
1278 24. Kidder BL, Hu G, Zhao K. KDM5B focuses H3K4 methylation near promoters and enhancers during
1279 embryonic stem cell self-renewal and differentiation. Genome Biol. 2014;15(2):R32. doi: 10.1186/gb-2014-15-2-
1280 r32. PubMed PMID: 24495580; PubMed Central PMCID: PMCPMC4053761.
1281 25. Dorna D, Paluszczak J. The Emerging Significance of Histone Lysine Demethylases as Prognostic Markers
1282 and Therapeutic Targets in Head and Neck Cancers. Cells. 2022;11(6). Epub 2022/03/26. doi:
1283 10.3390/cells11061023. PubMed PMID: 35326475; PubMed Central PMCID: PMCPMC8946939.
1284 26. Yang GJ, Zhu MH, Lu XJ, Liu YJ, Lu JF, Leung CH, et al. The emerging role of KDM5A in human
1285 cancer. J Hematol Oncol. 2021;14(1):30. Epub 2021/02/19. doi: 10.1186/s13045-021-01041-1. PubMed PMID:
1286 33596982; PubMed Central PMCID: PMCPMC7888121.
1287 27. Johansson C, Velupillai S, Tumber A, Szykowska A, Hookway ES, Nowak RP, et al. Structural analysis of
1288 human KDM5B guides histone demethylase inhibitor development. Nat Chem Biol. 2016;12(7):539-45. doi:
1289 10.1038/nchembio.2087. PubMed PMID: 27214403.
1290 28. LABELLE M, BOESEN T, KHAN Q, VAKITI RR, SHARMA U, YANG Y, et al., inventors
1291 INHIBITORS OF HISTONE DEMETHYLASES2016.
1292 29. LABELLE M, BOESEN T, MEHROTRA M, KHAN Q, ULLAH F, inventors INHIBITORS OF
1293 HISTONE DEMETHYLASES2015.
1294 30. AGUAYO E, APPLEBY T, BIRKUS G, CHENG G, DORNAN D, KOBAYASHI T, et al.,
1295 inventorsMETHODS OF TREATING HEPATITIS B VIRUS2016.
1296 31. Kramvis A. Genotypes and genetic variability of hepatitis B virus. Intervirology. 2014;57(3-4):141-50. doi:
1297 10.1159/000360947. PubMed PMID: 25034481.
1298 32. King ON, Li XS, Sakurai M, Kawamura A, Rose NR, Ng SS, et al. Quantitative high-throughput screening
1299 identifies 8-hydroxyquinolines as cell-active histone demethylase inhibitors. PLoS One. 2010;5(11):e15535. doi:
1300 10.1371/journal.pone.0015535. PubMed PMID: 21124847; PubMed Central PMCID: PMCPMC2990756.
1301 33. Mimasu S, Umezawa N, Sato S, Higuchi T, Umehara T, Yokoyama S. Structurally designed trans-2-
1302 phenylcyclopropylamine derivatives potently inhibit histone demethylase LSD1/KDM1. Biochemistry.
1303 2010;49(30):6494-503. doi: 10.1021/bi100299r. PubMed PMID: 20568732.
1304 34. Leupin O, Bontron S, Schaeffer C, Strubin M. Hepatitis B virus X protein stimulates viral genome
1305 replication via a DDB1-dependent pathway distinct from that leading to cell death. J Virol. 2005;79(7):4238-45. doi:
1306 10.1128/JVI.79.7.4238-4245.2005. PubMed PMID: 15767425; PubMed Central PMCID: PMCPMC1061538.
1307 35. Li T, Robert EI, van Breugel PC, Strubin M, Zheng N. A promiscuous alpha-helical motif anchors viral
1308 hijackers and substrate receptors to the CUL4-DDB1 ubiquitin ligase machinery. Nat Struct Mol Biol.
1309 2010;17(1):105-11. doi: 10.1038/nsmb.1719. PubMed PMID: 19966799; PubMed Central PMCID:
1310 PMCPMC2823288.
1311 36. Hodgson AJ, Hyser JM, Keasler VV, Cang Y, Slagle BL. Hepatitis B virus regulatory HBx protein binding
1312 to DDB1 is required but is not sufficient for maximal HBV replication. Virology. 2012;426(1):73-82. doi:
1313 10.1016/j.virol.2012.01.021. PubMed PMID: 22342275; PubMed Central PMCID: PMCPMC3294142.
1314 37. Decorsiere A, Mueller H, van Breugel PC, Abdul F, Gerossier L, Beran RK, et al. Hepatitis B virus X
1315 protein identifies the Smc5/6 complex as a host restriction factor. Nature. 2016;531(7594):386-9. doi:
1316 10.1038/nature17170. PubMed PMID: 26983541.

1317 38. Schoggins JW, Rice CM. Interferon-stimulated genes and their antiviral effector functions. Curr Opin
1318 Virol. 2011;1(6):519-25. doi: 10.1016/j.coviro.2011.10.008. PubMed PMID: 22328912; PubMed Central PMCID:
1319 PMCPMC3274382.
1320 39. Dandri M, Burda MR, Torok E, Pollok JM, Iwanska A, Sommer G, et al. Repopulation of mouse liver with
1321 human hepatocytes and in vivo infection with hepatitis B virus. Hepatology. 2001;33(4):981-8. Epub 2001/04/03.
1322 doi: 10.1053/jhep.2001.23314. PubMed PMID: 11283864.
1323 40. Ptaschinski C, Mukherjee S, Moore ML, Albert M, Helin K, Kunkel SL, et al. RSV-Induced H3K4
1324 Demethylase KDM5B Leads to Regulation of Dendritic Cell-Derived Innate Cytokines and Exacerbates
1325 Pathogenesis In Vivo. PLoS Pathog. 2015;11(6):e1004978. doi: 10.1371/journal.ppat.1004978. PubMed PMID:
1326 26083387; PubMed Central PMCID: PMCPMC4470918.
1327 41. Lawrence M, Daujat S, Schneider R. Lateral Thinking: How Histone Modifications Regulate Gene
1328 Expression. Trends Genet. 2016;32(1):42-56. doi: 10.1016/j.tig.2015.10.007. PubMed PMID: 26704082.
1329 42. Ladner SK, Otto MJ, Barker CS, Zaifert K, Wang GH, Guo JT, et al. Inducible expression of human
1330 hepatitis B virus (HBV) in stably transfected hepatoblastoma cells: a novel system for screening potential inhibitors
1331 of HBV replication. Antimicrob Agents Chemother. 1997;41(8):1715-20. PubMed PMID: 9257747; PubMed
1332 Central PMCID: PMCPMC163991.
1333 43. Livak KJ, Schmittgen TD. Analysis of relative gene expression data using real-time quantitative PCR and
1334 the 2(-Delta Delta C(T)) Method. Methods. 2001;25(4):402-8. doi: 10.1006/meth.2001.1262. PubMed PMID:
1335 11846609.
1336 44. Niu C, Livingston CM, Li L, Beran RK, Daffis S, Ramakrishnan D, et al. The Smc5/6 Complex Restricts
1337 HBV when Localized to ND10 without Inducing an Innate Immune Response and Is Counteracted by the HBV X
1338 Protein Shortly after Infection. PLoS One. 2017;12(1):e0169648. doi: 10.1371/journal.pone.0169648. PubMed
1339 PMID: 28095508; PubMed Central PMCID: PMCPMC5240991 does not alter our adherence to PLOS ONE policies
1340 on sharing data and materials.
1341 45. Tateno C, Yoshizane Y, Saito N, Kataoka M, Utoh R, Yamasaki C, et al. Near completely humanized liver
1342 in mice shows human-type metabolic responses to drugs. Am J Pathol. 2004;165(3):901-12. doi: 10.1016/S0002-
1343 9440(10)63352-4. PubMed PMID: 15331414; PubMed Central PMCID: PMCPMC1618591.
1344 46. Shinkai N, Matsuura K, Sugauchi F, Watanabe T, Murakami S, Iio E, et al. Application of a newly
1345 developed high-sensitivity HBsAg chemiluminescent enzyme immunoassay for hepatitis B patients with HBsAg
1346 seroclearance. J Clin Microbiol. 2013;51(11):3484-91. doi: 10.1128/JCM.00726-13. PubMed PMID: 23946517;
1347 PubMed Central PMCID: PMCPMC3889723.
1348 47. Yamasaki C, Kataoka M, Kato Y, Kakuni M, Usuda S, Ohzone Y, et al. In vitro evaluation of cytochrome
1349 P450 and glucuronidation activities in hepatocytes isolated from liver-humanized mice. Drug Metab Pharmacokinet.
1350 2010;25(6):539-50. PubMed PMID: 20930422.
1351 48. Deguchi M, Yamashita N, Kagita M, Asari S, Iwatani Y, Tsuchida T, et al. Quantitation of hepatitis B
1352 surface antigen by an automated chemiluminescent microparticle immunoassay. J Virol Methods. 2004;115(2):217-
1353 22. PubMed PMID: 14667538.
1354 49. Dobin A, Davis CA, Schlesinger F, Drenkow J, Zaleski C, Jha S, et al. STAR: ultrafast universal RNA-seq
1355 aligner. Bioinformatics. 2013;29(1):15-21. doi: 10.1093/bioinformatics/bts635. PubMed PMID: 23104886; PubMed
1356 Central PMCID: PMCPMC3530905.
1357 50. Robinson MD, McCarthy DJ, Smyth GK. edgeR: a Bioconductor package for differential expression
1358 analysis of digital gene expression data. Bioinformatics. 2010;26(1):139-40. doi: 10.1093/bioinformatics/btp616.
1359 PubMed PMID: 19910308; PubMed Central PMCID: PMCPMC2796818.
1360 51. Law CW, Chen Y, Shi W, Smyth GK. voom: Precision weights unlock linear model analysis tools for
1361 RNA-seq read counts. Genome Biol. 2014;15(2):R29. doi: 10.1186/gb-2014-15-2-r29. PubMed PMID: 24485249;
1362 PubMed Central PMCID: PMCPMC4053721.
1363 52. Benjamini Y, Hochberg Y. Controlling the False Discovery Rate: A Practical and Powerful Approach to
1364 Multiple Testing. J Roy Statist Soc Ser B (Methodological). 1995;57 289 - 300.
1365

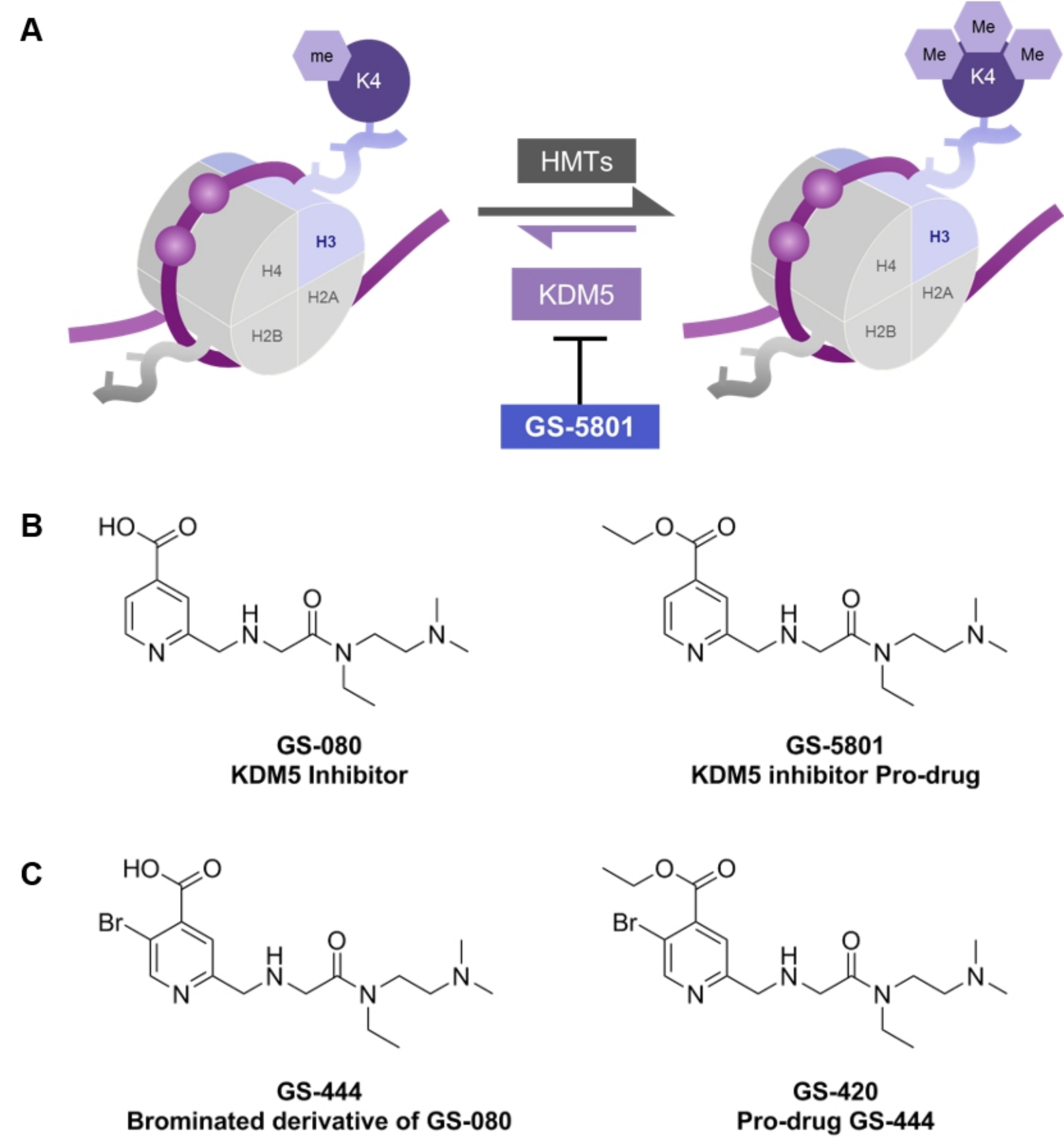
A
me
K4
H3
H4
H2A
H2B
HMTs
KDM5
GS-5801
Me
Me
Me
K4
H3
H4
H2A
H2B
B
GS-080
KDM5 Inhibitor
GS-5801
KDM5 inhibitor Pro-drug
C
GS-444
Brominated derivative of GS-080
GS-420
Pro-drug GS-444

Figure1

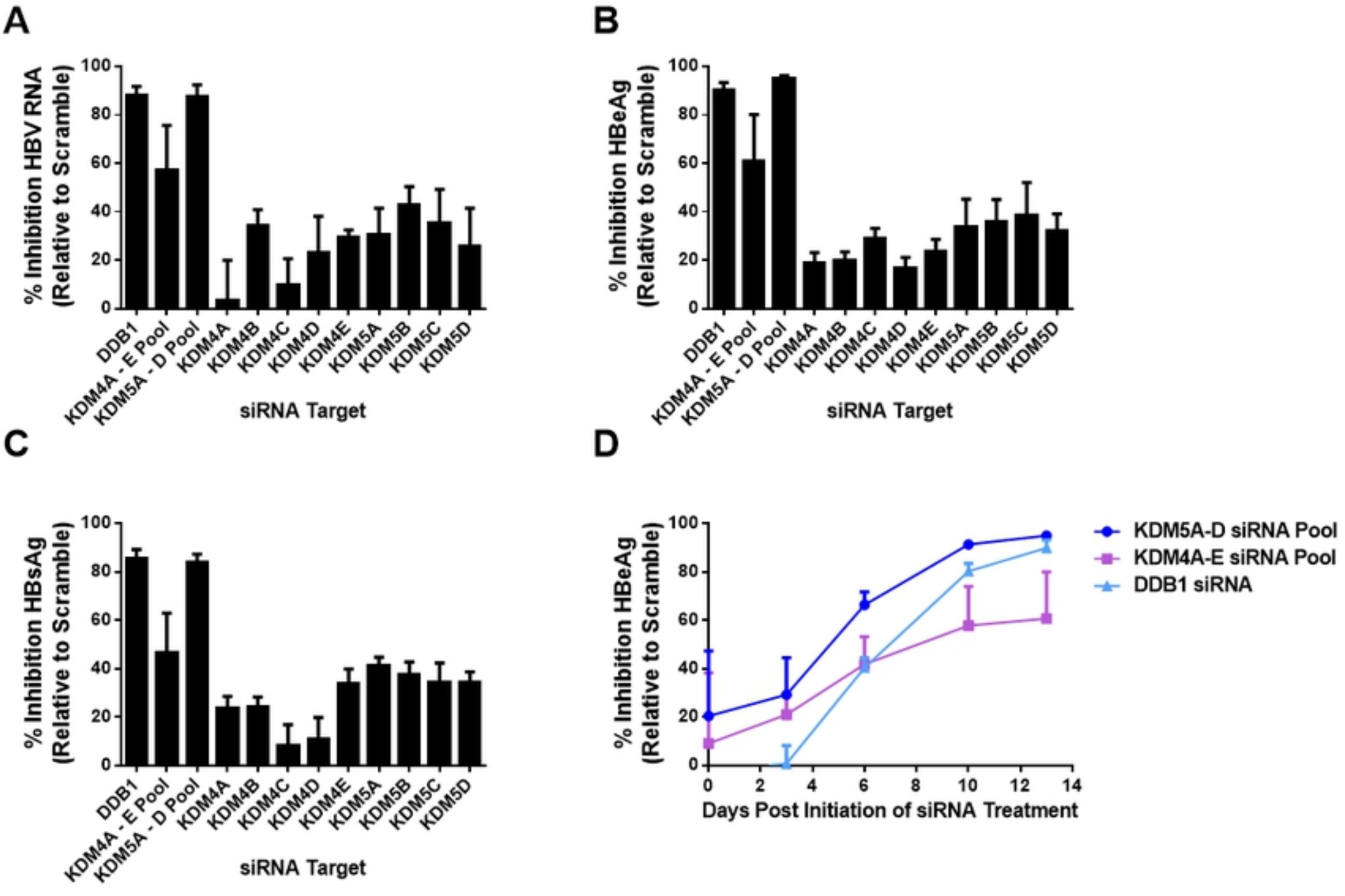
A
% Inhibition HBV RNA
(Relative to Scramble)
100
80
60
40
20
0
DDB1
KDM4A - E Pool
KDM5A - D Pool
KDM4A
KDM4B
KDM4C
KDM4D
KDM4E
KDM5A
KDM5B
KDM5C
KDM5D
siRNA Target
B
% Inhibition HBeAg
(Relative to Scramble)
100
80
60
40
20
0
DDB1
KDM4A - E Pool
KDM5A - D Pool
KDM4A
KDM4B
KDM4C
KDM4D
KDM4E
KDM5A
KDM5B
KDM5C
KDM5D
siRNA Target
C
% Inhibition HBsAg
(Relative to Scramble)
100
80
60
40
20
0
DDB1
KDM4A - E Pool
KDM5A - D Pool
KDM4A
KDM4B
KDM4C
KDM4D
KDM4E
KDM5A
KDM5B
KDM5C
KDM5D
siRNA Target
D
% Inhibition HBeAg
(Relative to Scramble)
100
80
60
40
20
0
0
2
4
6
8
10
12
14
Days Post Initiation of siRNA Treatment
KDM5A-D siRNA Pool
KDM4A-E siRNA Pool
DDB1 siRNA

Figure2

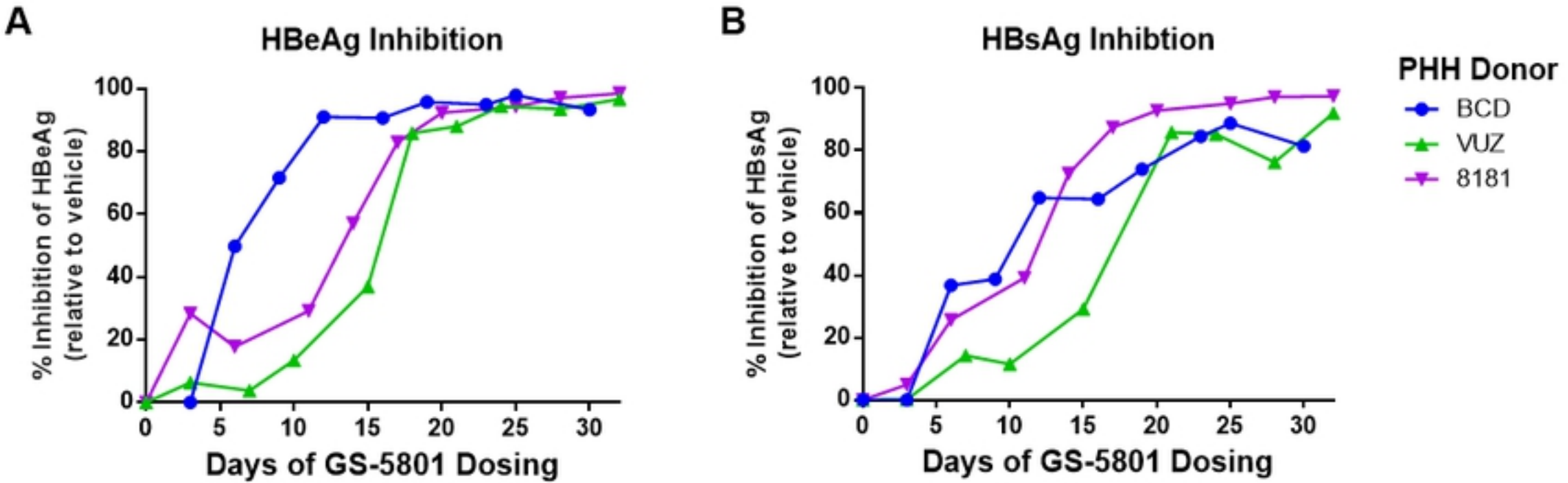
A
HBeAg Inhibition
% Inhibition of HBeAg (relative to vehicle)
100
80
60
40
20
0
0
5
10
15
20
25
30
Days of GS-5801 Dosing
B
HBsAg Inhibtion
% Inhibition of HBsAg (relative to vehicle)
100
80
60
40
20
0
0
5
10
15
20
25
30
Days of GS-5801 Dosing
PHH Donor
BCD
VUZ
8181

Figure3

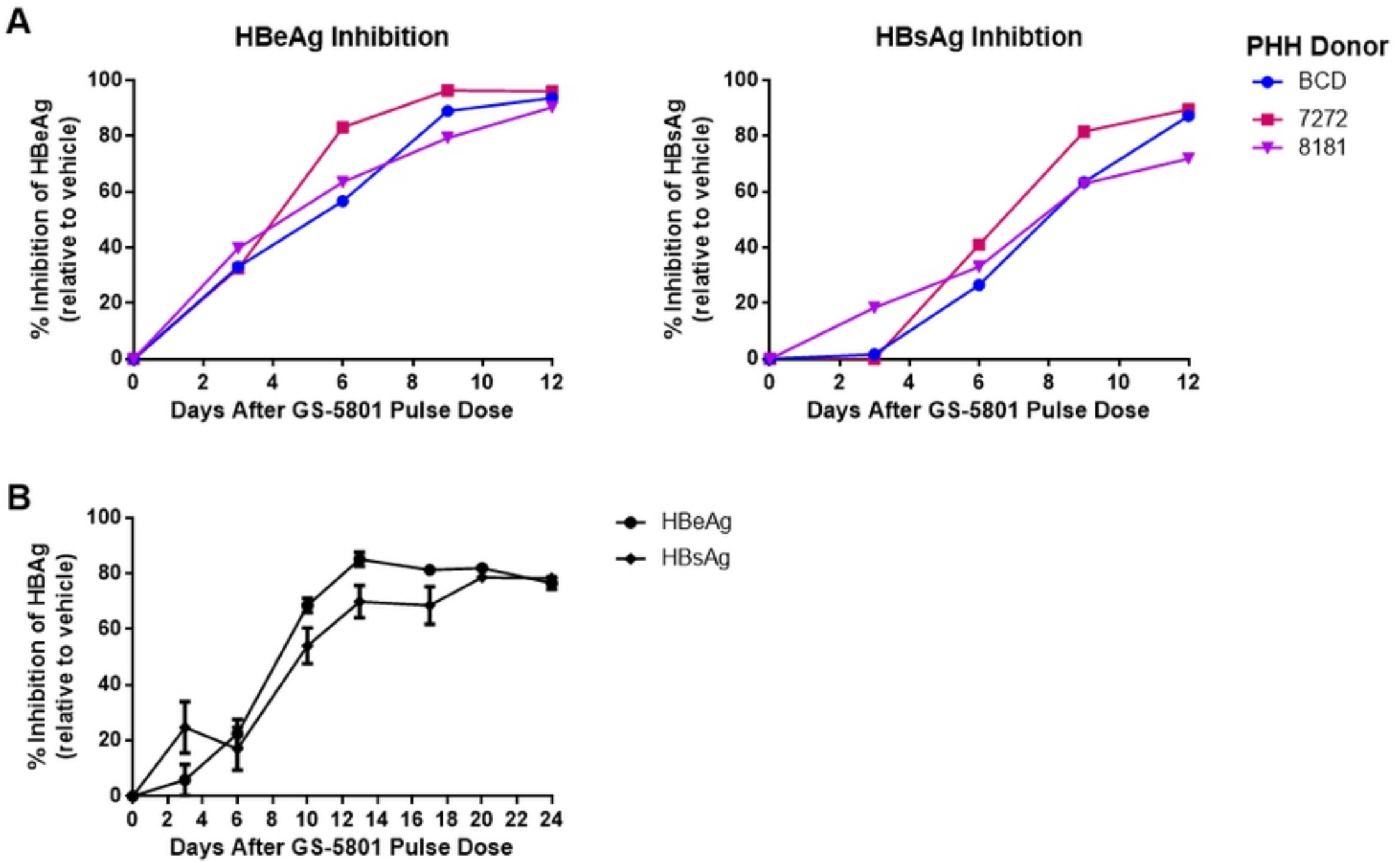
A
HBeAg Inhibition
% Inhibition of HBeAg (relative to vehicle)
Days After GS-5801 Pulse Dose
HBsAg Inhibtion
% Inhibition of HBsAg (relative to vehicle)
Days After GS-5801 Pulse Dose
PHH Donor
BCD
7272
8181
B
% Inhibition of HBAg (relative to vehicle)
Days After GS-5801 Pulse Dose
HBeAg
HBsAg

Figure4

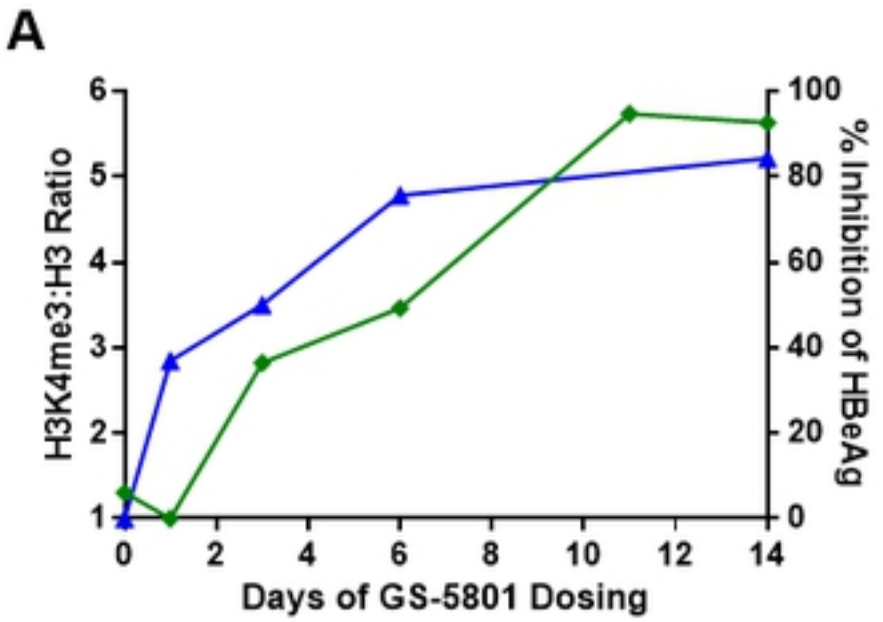

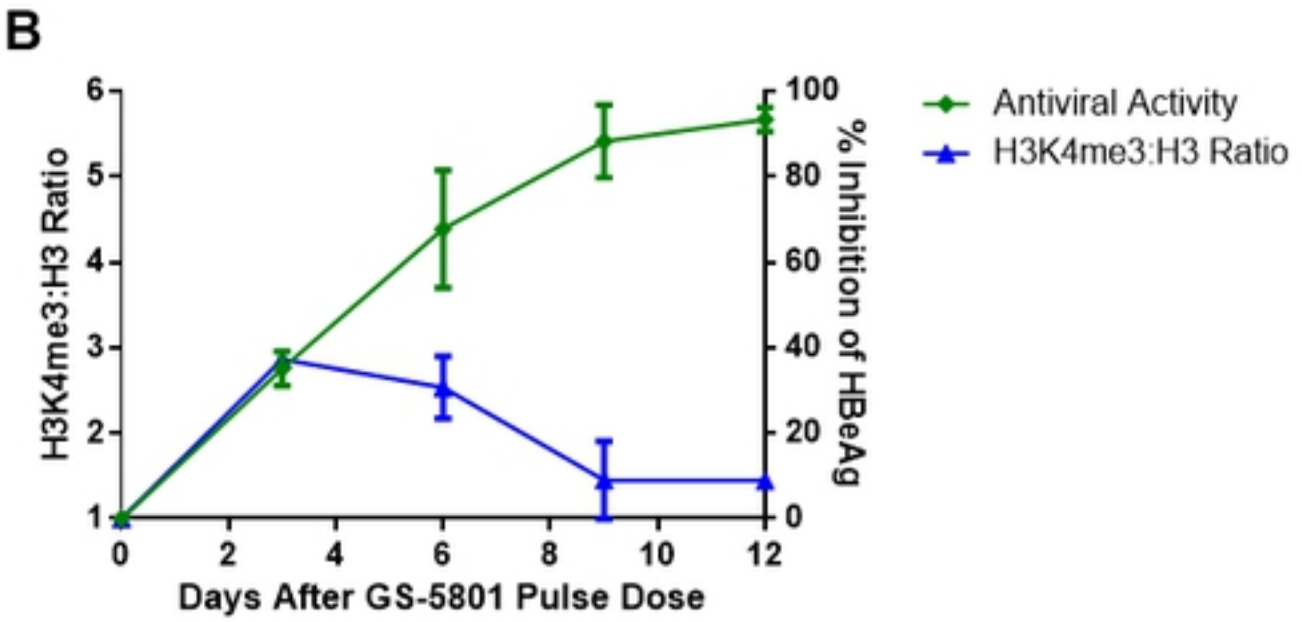

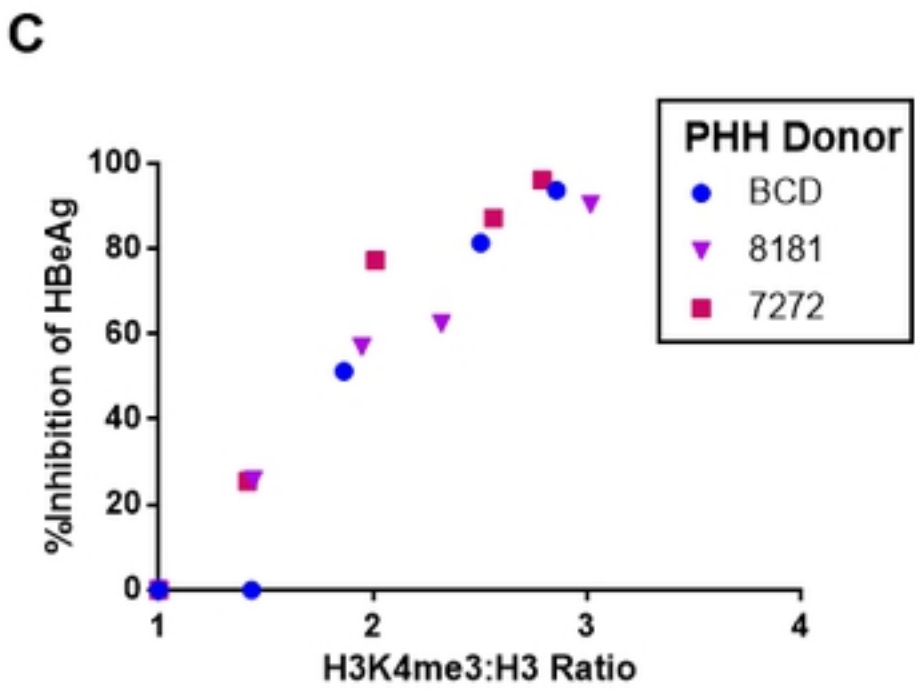

PHH Donor	r value	p value
BCD	0.97	0.0065
8181	0.99	0.0021
7272	0.97	0.0052

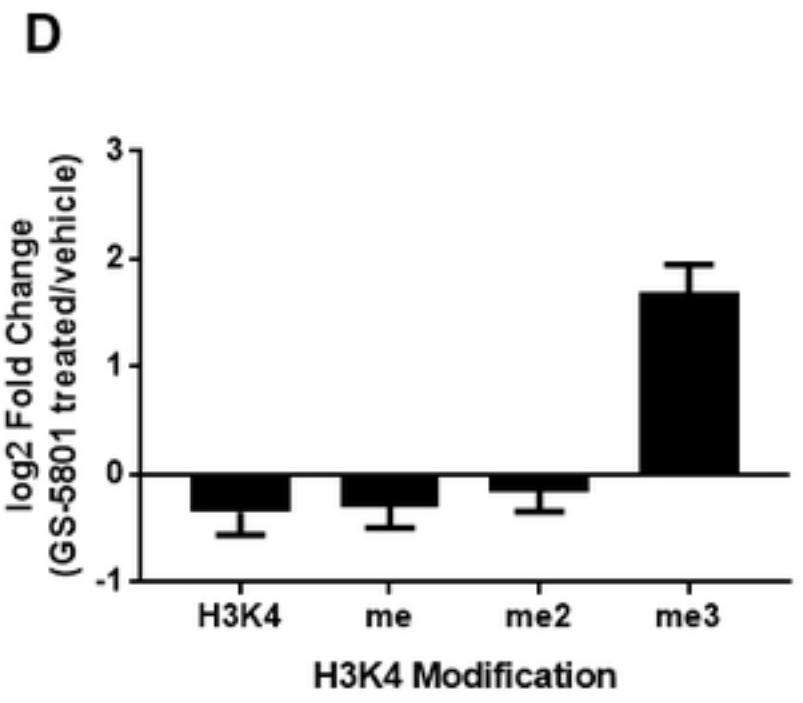

Figure5

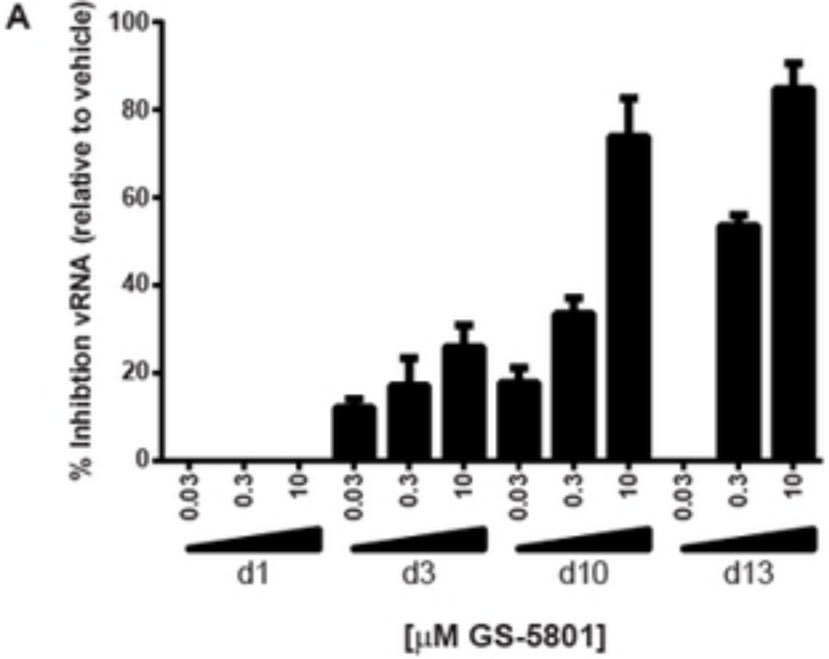
A
% Inhibition vRNA (relative to vehicle)
100
80
60
40
20
0
0.03
0.3
10
d1
d3
d10
d13
[μM GS-5801]

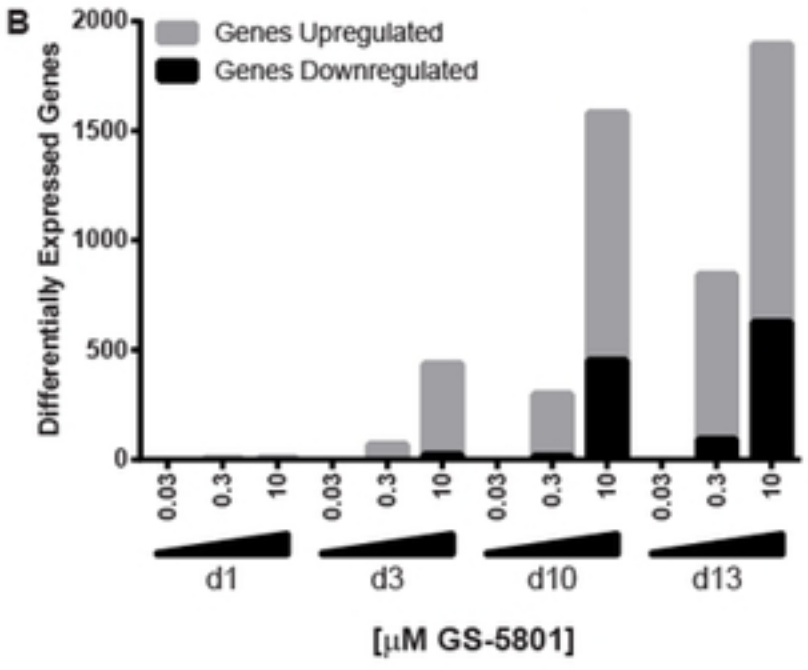
B
Genes Upregulated
Genes Downregulated
Differentially Expressed Genes
2000
1500
1000
500
0
0.03
0.3
10
d1
d3
d10
d13
[μM GS-5801]

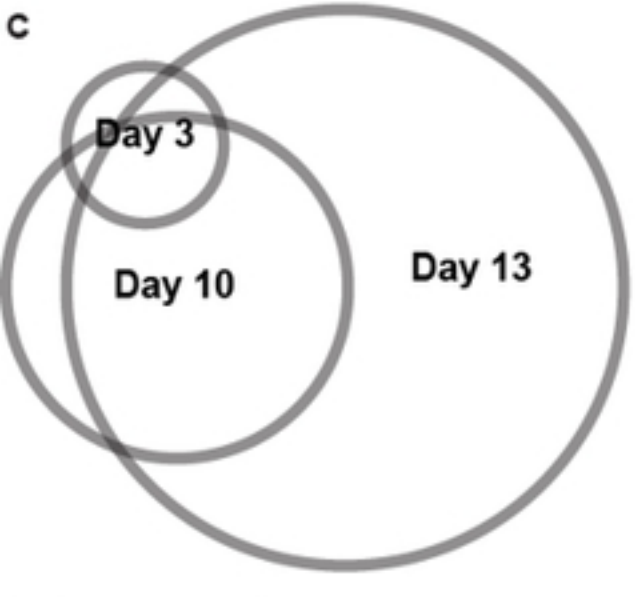
C
Day 3
Day 10
Day 13

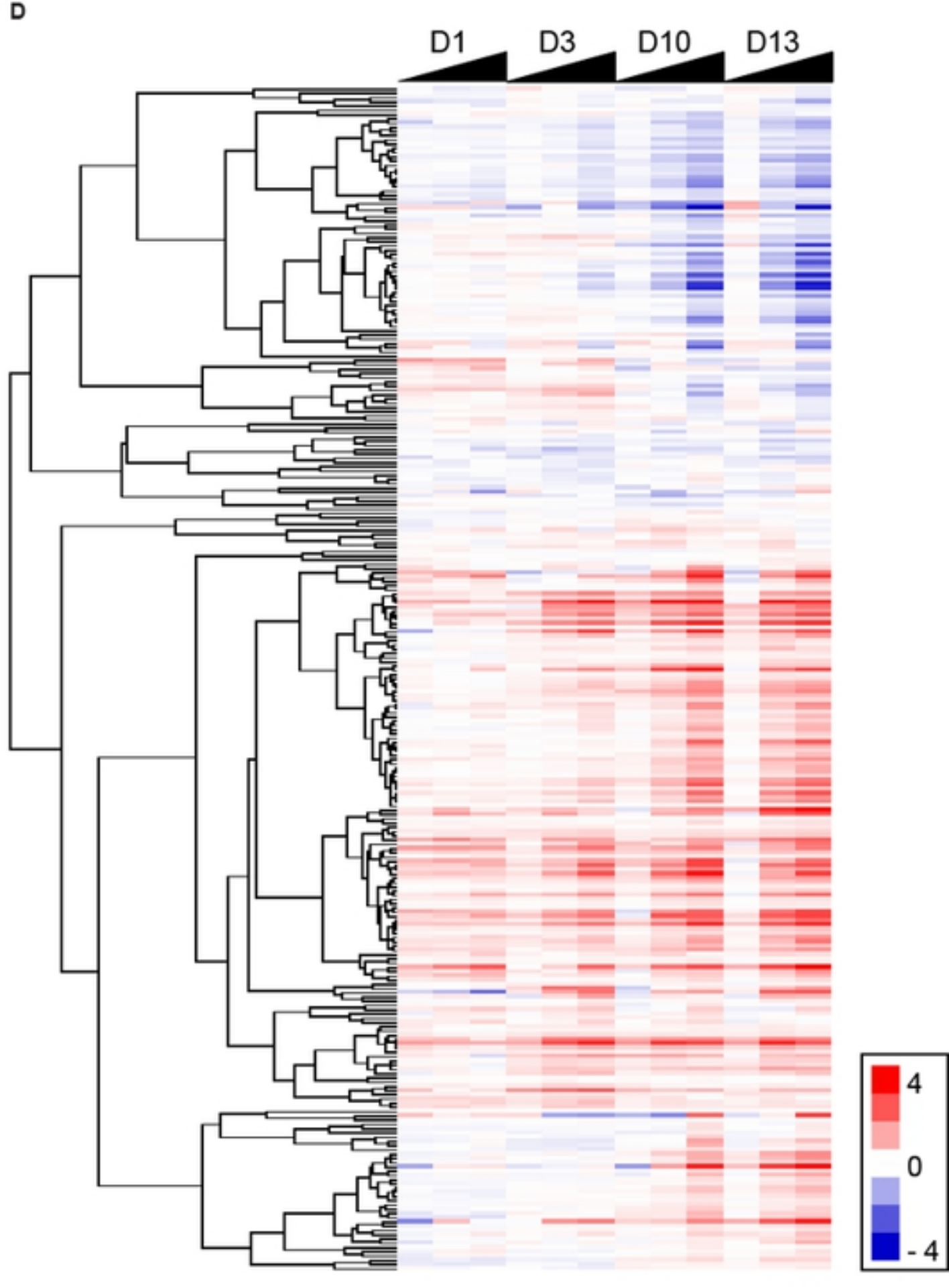
D
D1
D3
D10
D13
4
0
- 4

Figure6

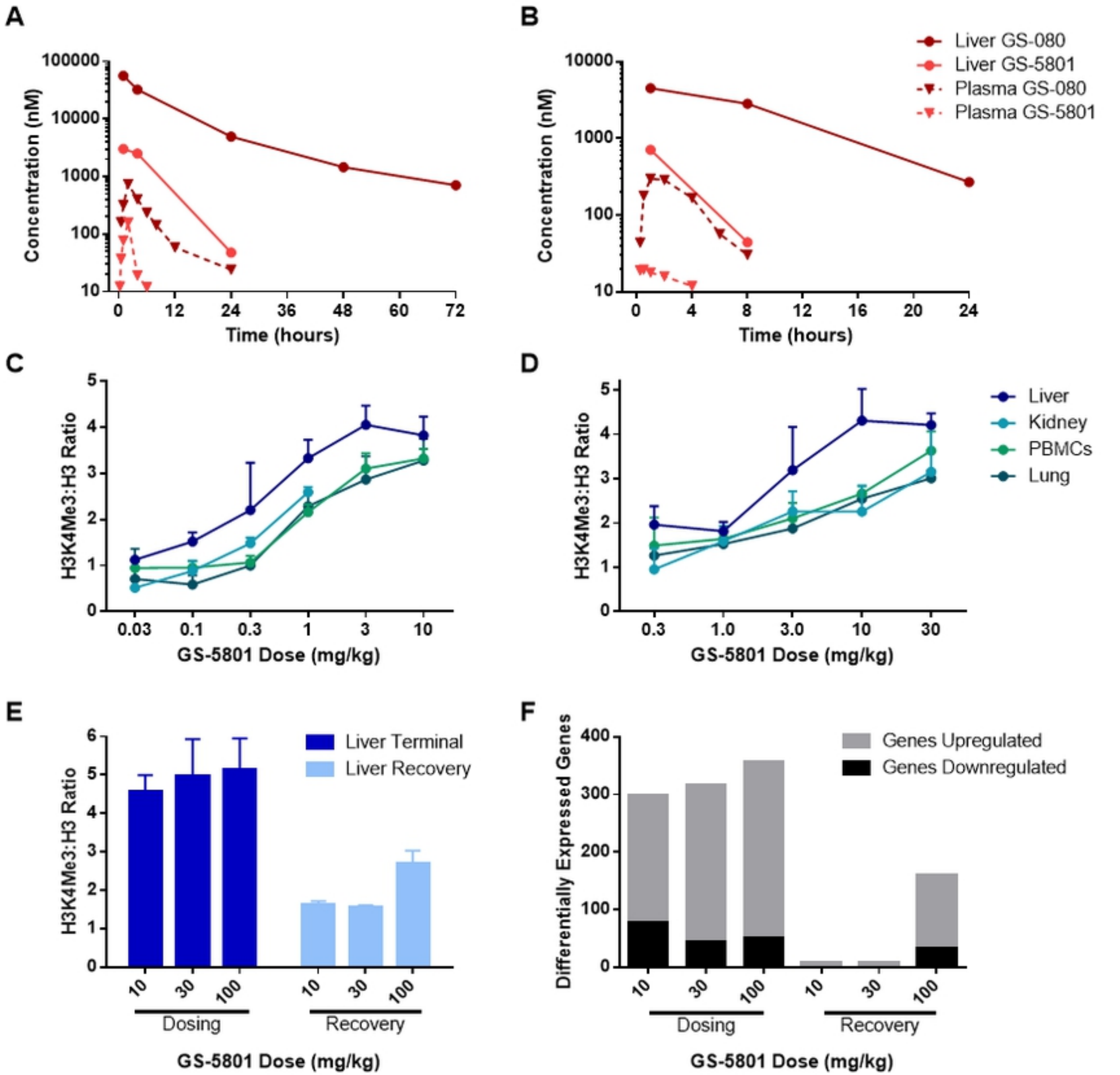
A
Concentration (nM)
Time (hours)
B
Liver GS-080
Liver GS-5801
Plasma GS-080
Plasma GS-5801
Concentration (nM)
Time (hours)
C
H3K4Me3:H3 Ratio
GS-5801 Dose (mg/kg)
D
Liver
Kidney
PBMCs
Lung
H3K4Me3:H3 Ratio
GS-5801 Dose (mg/kg)
E
Liver Terminal
Liver Recovery
H3K4Me3:H3 Ratio
Dosing
Recovery
GS-5801 Dose (mg/kg)
F
Genes Upregulated
Genes Downregulated
Differentially Expressed Genes
Dosing
Recovery
GS-5801 Dose (mg/kg)

Figure7

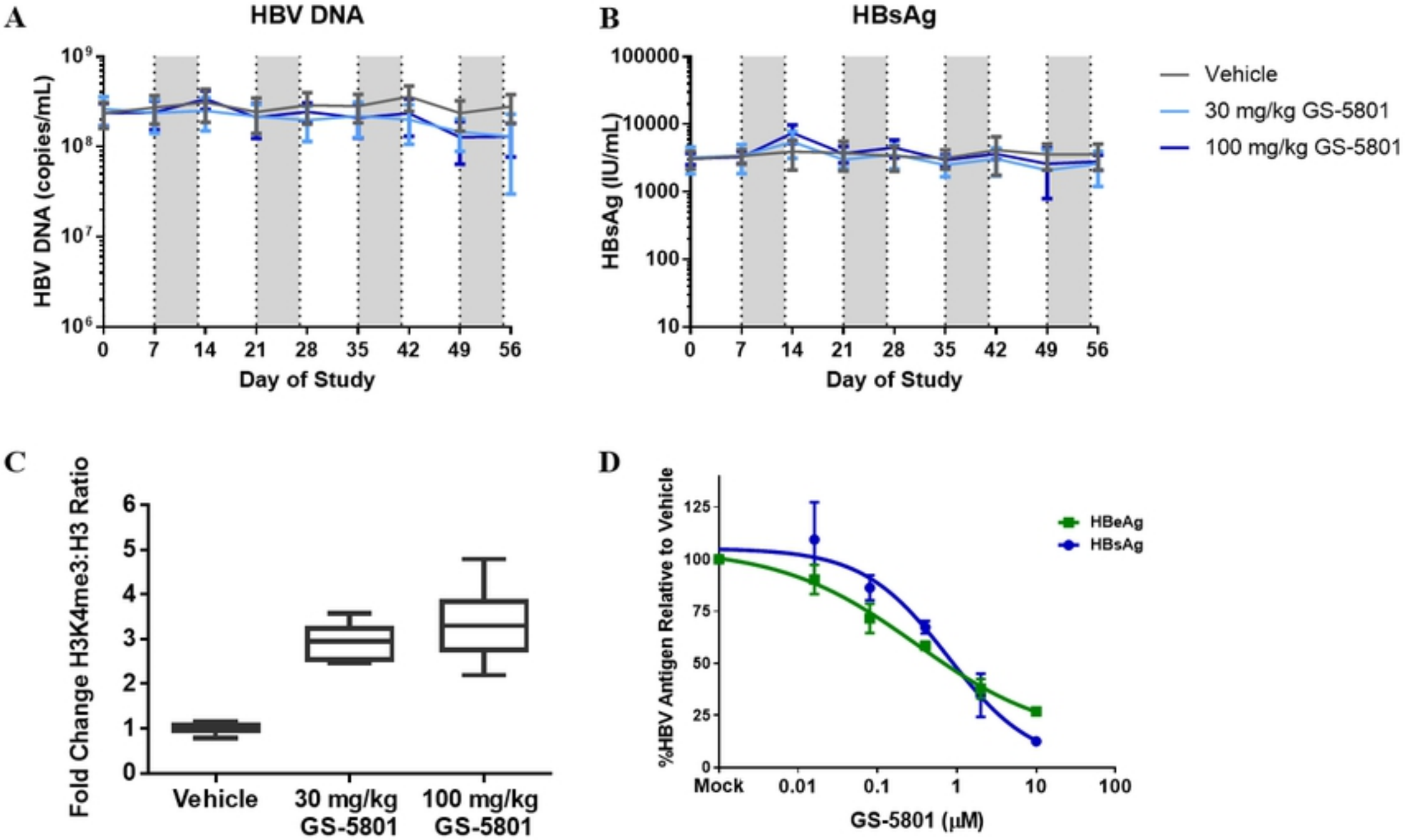
A
HBV DNA
HBV DNA (copies/mL)
Day of Study
B
HBsAg
HBsAg (IU/mL)
Day of Study
Vehicle
30 mg/kg GS-5801
100 mg/kg GS-5801
C
Fold Change H3K4me3:H3 Ratio
Vehicle
30 mg/kg GS-5801
100 mg/kg GS-5801
D
%HBV Antigen Relative to Vehicle
HBeAg
HBsAg
GS-5801 (μM)

Figure8